MASTER

Measurement and modelling of the high frequency reginition behaviour of vacuum interrupters with various contact materials

Dirven, R.G.C.

Award date:
1993

EG/93/677

FACULTEIT DER ELEKTROTECHNIEK

Vakgroep Elektrische Energiesystemen

MEASUREMENT AND MODELLING OF THE HIGH FREQUENCY REGINITION BEHAVIOUR OF VACUUM INTERRUPTERS WITH VARIOUS CONTACT MATERIALS

R.G.C. Dirven

EG/93/677

Coached by: Dr.ir. R.P.P. Smeets
Professor: Prof.Ir. G.C. Damstra

Eindhoven, June 1993

EINDHOVEN UNIVERSITY OF TECHNOLOGY

SUMMARY

In medium voltage circuits, there is an increasing use of vacuum interrupters (about 50% world wide). In vacuum interrupters, high and/or steep overvoltages may be caused by voltage escalation and virtual current chopping due to (multiple) reignitions followed by a high frequency (500kHz) current. The appearance and duration of reignitions is determined by an interaction between parasitic circuit components and interrupter. The interrupter behaviour (dielectric strength, high frequency (HF) current interruption capability) is mainly determined by the contact material and the opening speed. The aim of the research described in this report is to investigate the interrupter behaviour by measurement and modelling for a medium voltage type of vacuum circuit breaker with six different contact materials: Cu, CuCr, AgWC, CuW, CuBi and CuTeSe.

For measurement of the reignition phenomena a synthetic circuit is used. Electromagnetic shielding precautions were made to be able to do proper voltage measurements in the magnetic field caused by the HF-current. During several measurements, the dielectric recovery was measured and it was found that the HF-current interruption capability can be described by a combination of dielectric and thermal behaviour of the vacuum gap. This description turned out to be much better than the commonly accepted maximum interruptable di/dt. The dielectric behaviour is closely related to the cold dielectric strength. The occurrence of thermal behaviour sets in above a threshold value of the HF-current amplitude. For the measurements done, the dielectric behaviour was dominant. Therefore the contact materials that show good dielectric strength are also succesfull in interrupting the HF-current.

Both dielectric and thermal behaviour are integrated in a model presented, which can be used for simulation of a vacuum interrupter in a complete inductive circuit.

CONTENTS

1. INTRODUCTION 4

2. VACUUM CIRCUIT BREAKERS IN INDUCTIVE CIRCUITS 6
2.1 Overvoltages in an inductive circuit 6
2.2 Interrupter parameters 8
2.2.1 The chopping current 8
2.2.2 The dielectric recovery 8
2.2.3 The high frequency current interruption capability 8
2.3 The breakdown voltage reduction factor 11

3. EXPERIMENTS 14
3.1 The synthetic circuit 14
3.2 The measuring process 15
3.3 Voltage measurement problems 18
3.4 Definitions 20

4. RESULTS 22
4.1 The dielectric recovery 22
4.2 Reignition types 25
4.3 The high frequency interruption capability 26

5. MODELLING 32
5.1 The high frequency current interruption capability 32
5.2 The HF-current interruption model 33
5.3 The maximum interruptable di/dt 40
5.4 The simulation methods 41

6. CONCLUSIONS 42

7. RECOMMENDATIONS FOR FURTHER RESEARCH 44

8. REFERENCES 45

Appendix A: Equipment used 46

Acknowledgement 47

1. INTRODUCTION

In an electrical supply system, interrupters are very important for switching load and for protection. One type of interrupter is a vacuum circuit breaker (VCB), which is mostly used in medium voltage circuits (1-50kV). In 1965, GEC announced the availability of the world's first 3.3kV, 300A vacuum contactor, incorporating glass enveloped vacuum interrupters.

The advantages of switching a current in a vacuum, as opposed to air or oil, have been appreciated since the turn of the century. When the contacts of a VCB open, the arc is formed from vapourized contact material, and continues to burn only until the first current zero appears in the ac waveform. At this instant, the arc ceases, the metal vapour deionizes, cools and condenses, and the gap quickly reverts to an area of high dielectric strength able to withstand the recovery voltage. As the arcing period normally does not exceed one half cycle and the arc voltage is very low, the energy of the vacuum arc is therefore much less than that of arcs in air or oil and the contacts suffer far less wear than those in air or oil.

However, when ac current zero appears shortly after contact separation (< 1ms), there may be not enough dielectric strength to withstand the recovery voltage, and the interrupter reignites. This is especially the case for inductive currents, for example switching off stalled motors or no-load transformers, because there is a maximum voltage at the moment of current zero. At the moment of reignition a high frequency (HF) reignition current, caused by parasitic capacitances (cables) and inductances (cables, busbar) will flow through the interrupter again. During this reignition the connection between source and load is restored and the load current continues. If the current is interrupted, the recovery voltage may exceed the dielectric strength again, which results in multiple reignitions. The increasing load energy during the multiple reignitions causes voltage escalation in the circuit; overvoltages of many times the rated voltage are possible. Multiple reignitions can also cause current interruption in the adjacent phase (virtual current chopping), resulting in unacceptable overvoltages in the system. The appearance of multiple reignitions with virtual current chopping can be seen in figure 1.

The appearance of voltage escalation and virtual current chopping is highly dependant on the interaction of interrupter and circuit, which is illustrated in figure 2. For vacuum interrupters, the contact material is the dominant factor for the interrupter behaviour. Other influential factors are the delay time between the successive opening of the three poles and the contact opening speed. The aim of the research described in this report is to measure the dielectric recovery and the interrupter parameters which determine the high frequency reignition behaviour for a medium voltage type of VCB with six different contact materials: Cu, CuCr, AgWC, CuW, CuBi and CuTeSe. Further, it will be tried to classify various types of HF-reignitions and to identify criteria for HF-current interruption for use in simulation programs to estimate the probability of occurrence of multiple reignition/virtual chopping overvoltages in realistic circuits.

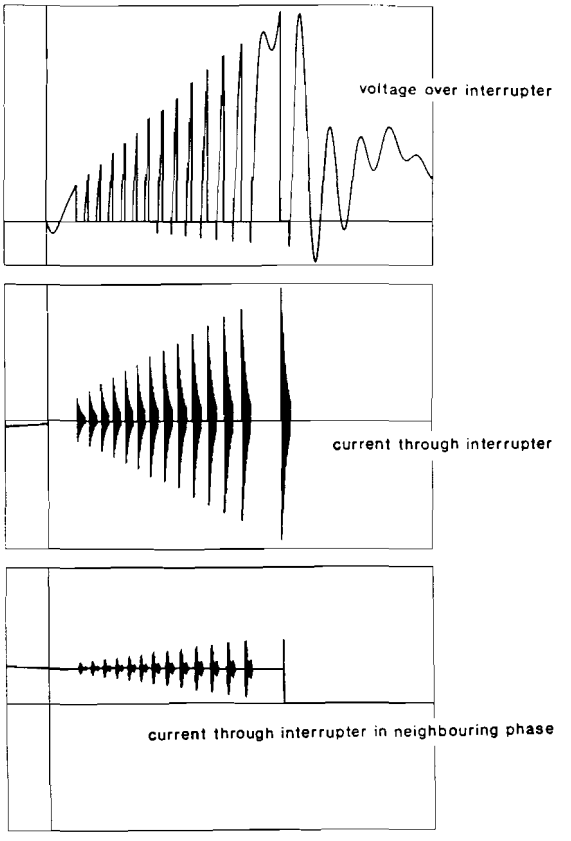

figure 1: multiple reignitions with virtual current chopping

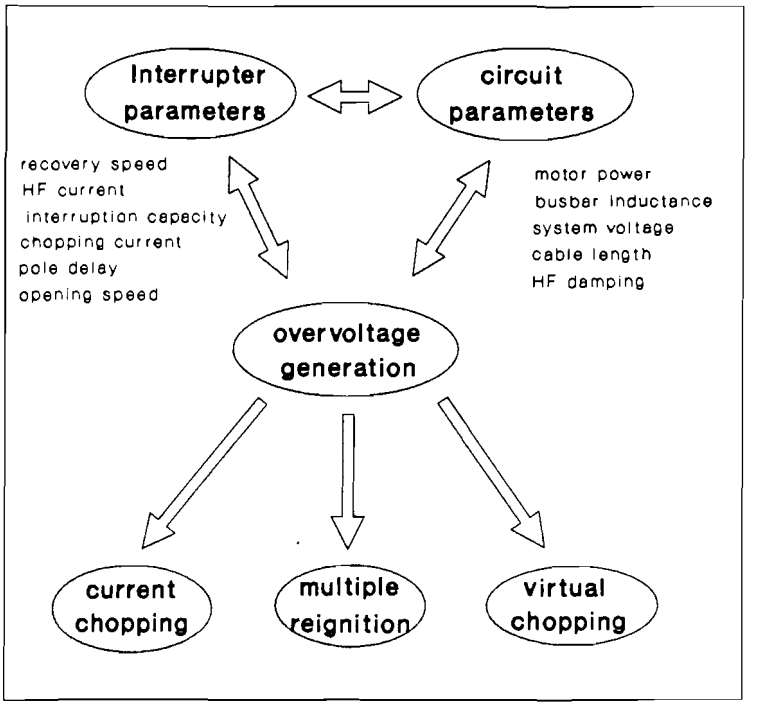

figure 2: interaction of interrupter and circuit

2. VACUUM CIRCUIT BREAKERS IN INDUCTIVE CIRCUITS

Last years there has been an increasing use of vacuum circuit breakers (VCB) in medium voltage circuits (1-50kV), especially for switching motors. The disadvantage of a VCB is the possible generation of high overvoltages, mostly in inductive circuits. Therefore, the attention in this report goes out to inductive circuits.

2.1 Overvoltages in an inductive circuit

When using VCBs in a strongly inductive circuit different overvoltages can appear. This can be seen from figure 3, a representation of a single phase inductive circuit.

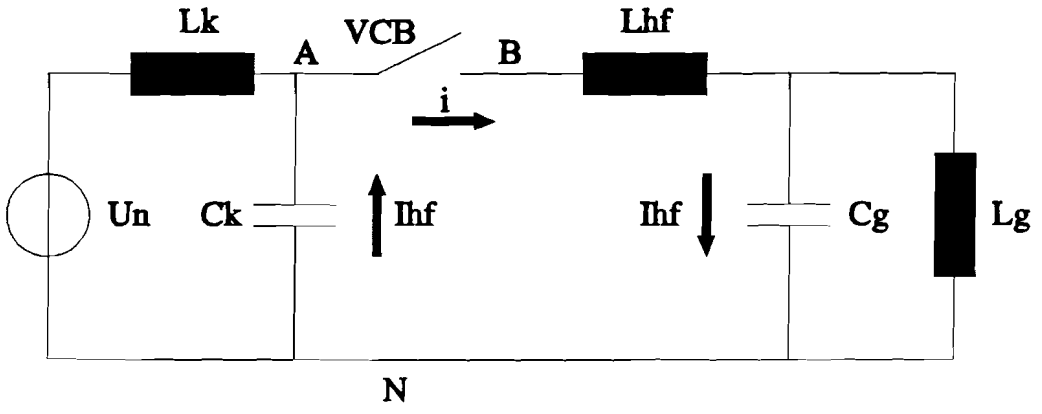

figure 3: a single phase inductive circuit

The source side consists of U_n, L_k and C_k. U_n and L_k represent the power source and its inductance, C_k the capacitance of parallel cables, busbar or compensation capacitance. The load side is formed by C_g and L_g, which represent the capacitance of the cable from interrupter to load and the inductive load, respectively. These two parts are coupled by the VCB. After contact separation, at the moment of current zero, the arc extinguishes and the dielectric strength of the interrupter has reached a certain level. This can be described by for example a linear function:

$$U_b = U_{b0} + S t_b \qquad (1)$$

where U_{b0} is the initial breakdown voltage, t_b is the time from the moment of contact separation, S is the recovery speed of the interrupter which is a function of the electrical field strength E_b and the opening speed v_0:

$$S = E_b v_0 \qquad (2)$$

At the moment of arc extinction both parts of the circuit are separated. The source side voltage of the circuit will oscillate with a frequency of $\omega_{ds} = 1/(L_k C_k)^{1/2}$ to U_n, the load part voltage with a frequency of $\omega_{dl} = 1/(L_g C_g)^{1/2}$ to zero. Thus the voltage over the gap, U_{AN}-U_{BN}, consists of these two frequencies in combination with the supply voltage and is called Transient Recovery Voltage (TRV).

When a 'strong' source side is considered, $L_k \ll L_g$, there will be an oscillation only in the load part at the moment of interruption. This can be seen in figure 4 [1]. The maximum of the TRV (U_{AB}) is reached at $t=t_m$.

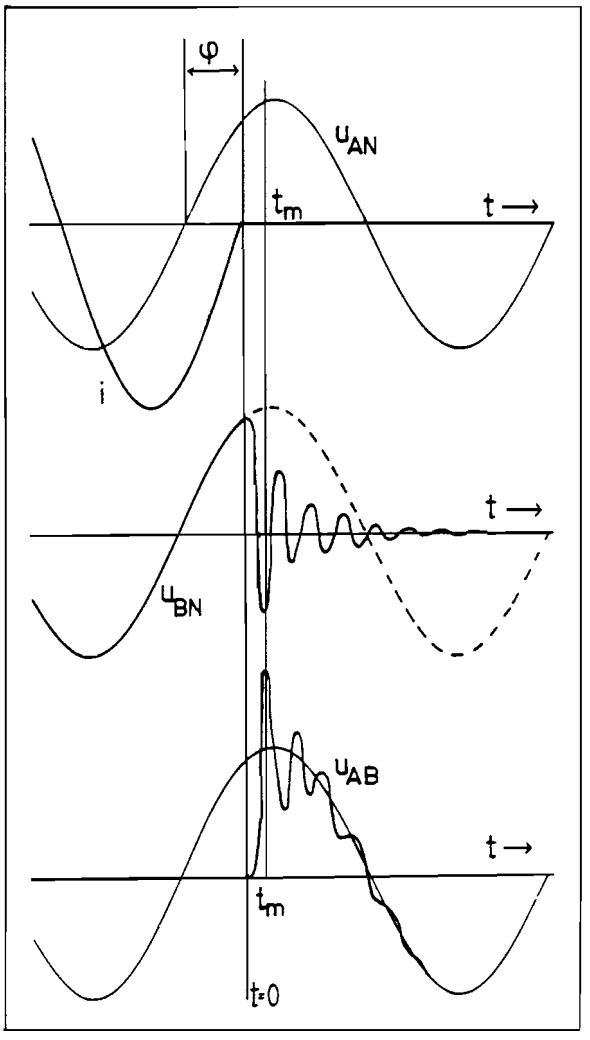

The reason for looking at inductive circuits is the maximum voltage that can appear at C_g at the moment of current zero, which causes the maximum of the TRV.

figure 4: TRV for a strong source side

VCBs normally interrupt just before current zero. The value of the current at this moment is called chopping current (I_{ch}). Compared to interruption at current zero, this causes an increase of energy in the load at the moment of interruption, so the maximum of U_{BN} increases too. This can be seen from:

$$\frac{1}{2}C_g U_{BN,\max}^2 = \frac{1}{2}C_g U_{chop}^2 + \frac{1}{2}L_g I_{ch}^2 \qquad (3)$$

So the maximum voltage over C_g is:

$$U_{BN,\max} = \sqrt{U_{chop}^2 + I_{ch}^2 Z_0^2} \qquad (4)$$

where

$$Z_0 = \sqrt{\frac{L_g}{C_g}} \tag{5}$$

and U_{chop} is U_{BN} at the moment of current interruption, so $U_{chop} \approx \hat{u}_n$.

2.2 Interrupter parameters

The appearance of overvoltages is the effect of an interaction between circuit and VCB. The interrupter parameters represent the behaviour of the interrupter itself. In this report only interrupter parameters will be discussed. More about the circuit parameters can be found in [2], [3] and [4]. In [2] it is concluded that the phenomena in VCBs can be accurately simulated, but 'a problem for application is not the simulation but the unknown interrupter parameters'. These parameters will be discussed here.

2.2.1 The chopping current

As mentioned before, VCBs normally interrupt just before current zero. The value of the current at this moment is called chopping current (I_{ch}) and is mainly determined by the contact material. The chopping current is considered to be a well known quantity.

2.2.2 The dielectric recovery

The dielectric recovery is already described by (1) on page 6. In combination with (2) it can be seen that S is determined by the mechanical opening speed (v_0) and the contact material (E_b). U_{b0} is also determined by the contact material. If the TRV exceeds the momentary value of U_b a reignition appears. The dielectric recovery at small gap lengths will be investigated experimentally in chapter 3.

2.2.3 The high frequency current interruption capability

High frequency (HF) phenomena play an important role in reignitions of VCBs. For HF-phenomena, the relevant part of figure 3 on page 6 is shown in figure 5, which exists of C_k, the VCB, L_{hf} and C_g. The parasitic capacitance of the interrupter is represented by C_p (order of 20pF), the inductance and the HF-damping of this circuit by L_{hf} (few tens of μH) and R_{hf} (2-4Ω) respectively.

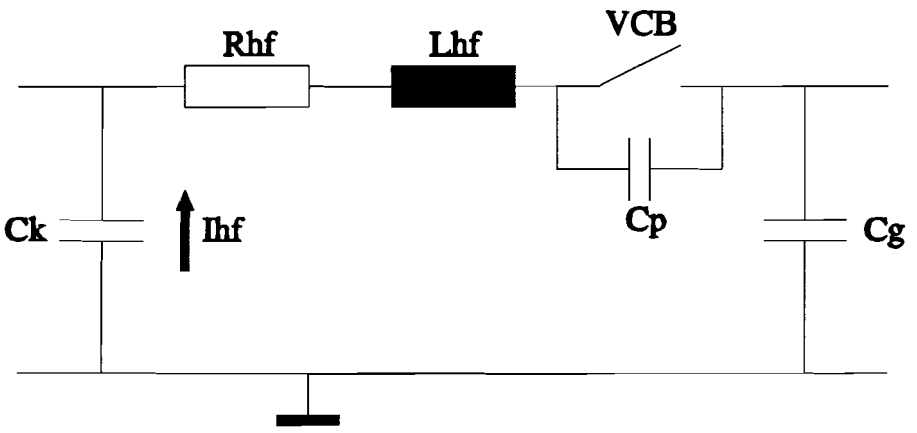

figure 5: part of single phase circuit relevant for HF-phenomena

figure 6 shows the expected high frequency voltage and current for the VCB.

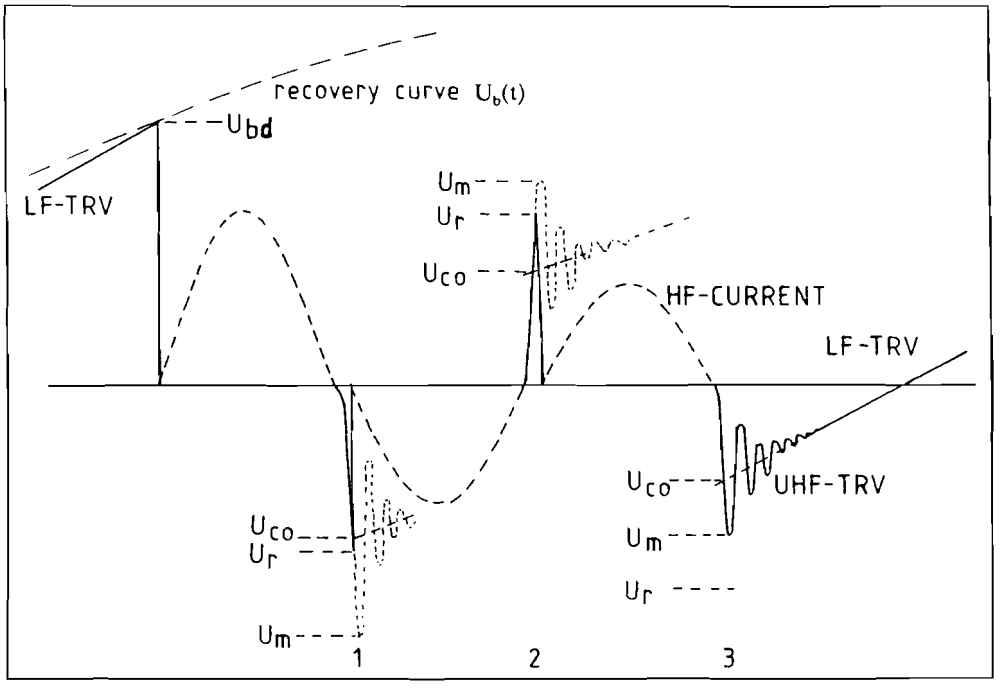

figure 6: high frequency reignitions in VCB

The dielectric recovery curve is described by $U_b(t)$ (dashed line). The TRV (U_{AB}) in figure 4 is the so called LF-TRV (as shown in figure 6), because its frequency is essentially low (few kHz) compared to the HF-current (few hundreds of kHz). When the LF-TRV exceeds the dielectric recovery curve, a breakdown appears and both capacitors are reconnected. The breakdown voltage is called U_{bd}. C_g has been discharging while C_k is still on the supply voltage (see U_{AN} and U_{BN} in figure 4 on page 7). The voltage difference is called U_{c0}. Both capacitors tend to reach the same voltage ($U_{c0}=0$), which causes a HF-current. This is illustrated in figure 7, where a simplified version of figure 5 is shown.

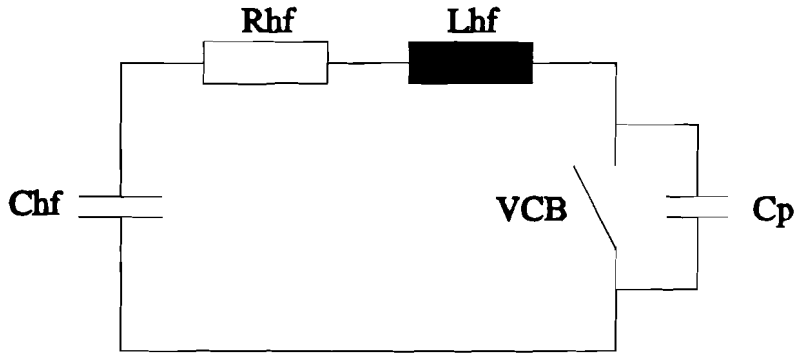

figure 7: simplified circuit for HF-phenomena

From figure 7 it can be seen that the HF-current frequency f is determined by:

$$f = \frac{1}{2\pi\sqrt{L_{hf}C_{hf}}} \tag{6}$$

where:

$$C_{hf} = \frac{C_k C_g}{C_k + C_g} \tag{7}$$

At the first HF-current zero ('1' in figure 6) U_{c0} is decreased because of HF-damping:

$$U_{c0} = U_{bd}\exp\left(-\frac{T}{2\tau}\right) \tag{8}$$

where

$$T = f^{-1} = 2\pi\sqrt{L_{hf}C_{hf}} \quad and \quad \tau = \frac{2L_{hf}}{R_{hf}} \tag{9}$$

The TRV will now rise to the value of U_{c0}, but because of C_p and L_{hf}, the TRV contains an ultra high frequency component (UHF-TRV) of a few MHz and will reach a maximum of U_m:

$$U_m = f_p U_{c0} \tag{10}$$

where f_p is the overshoot factor (f_p = 1.54 in the circuit used). If the UHF-TRV exceeds the momentary value of the breakdown voltage U_r, there is a new reignition and a new half period of HF-current. U_r is called 'reignition voltage'. This phenomenon is repeated at the second HF-current zero ('2'). Now U_{c0} has decreased again and the reignition voltage has increased because of the smaller HF-current, which will be explained in 2.3. From (8) it follows for the n^{th} HF-current zero:

$$U_{c0} = U_{bd} \exp\left(-\frac{nT}{2\tau}\right) \tag{11}$$

where n = the number of half HF-current periods. At the third HF-current zero ('3'), the UHF-TRV does not exceed U_r anymore and the HF-current is interrupted.

While the UHF-TRV is damped out, the voltage over the gap rises again because of the LF-TRV. If this LF-TRV exceeds the recovery curve again, the described phenomenon of reignitions and HF-current will be repeated. This process is called 'multiple reignition'. For studying this process of multiple reignitions with possible virtual current chopping, it is important to know when a reignition will appear (dielectric recovery) and for how long the HF-current will continue, which is determined by the interruption capability. This is because in real circuits, power frequency current is charging the inductive load during the period of HF arcing, thus increasing the stored energy in the load. Other than by the commonly accepted parameter of maximum interruptable di/dt, the interruption capability is described by a new parameter. This parameter is called 'breakdown voltage reduction factor' and is explained in 2.3.

2.3 The breakdown voltage reduction factor

From 2.2 it follows that for continuation of the HF arcing the (prospective) maximum value of the UHF-TRV (U_m) and the reignition voltage U_r have to be considered. Both U_m and U_r are considered to be absolute values. Thus an alternative criterion for HF-current interruption is stated by:

$$U_m < U_r \tag{12}$$

As can be seen from figure 6 on page 9 it is supposed that U_r is lower than the momentary value of the dielectric recovery curve ($U_b(t)$, dashed line), based on the expectation that the dielectric strength of the vacuum gap is reduced by the preceding HF-current because of thermal effects [5]. This reduction can be expressed by the 'breakdown voltage reduction factor' α [4]:

$$\alpha = \frac{U_r}{U_b} = \alpha_0 f(i_l) \tag{13}$$

where i_l is the precedent HF-current amplitude and α_0 is a constant. The current dependence of α is illustrated in figure 8. In theory: $0 \leq \alpha \leq 1$, so $\alpha_0 \leq 1$. A so called 'soft' metal has a low α and thus a low interruption capability for HF-currents. A 'hard' metal has a factor α close to 1.

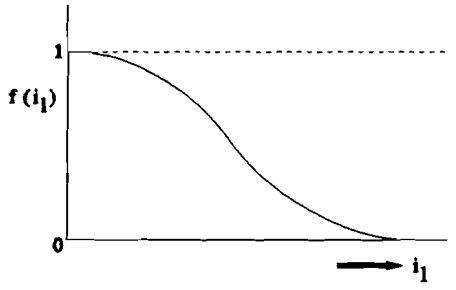

figure 8: current dependence of α

It is assumed that after a certain period of time (for example 5μs) the gap is recovered from the HF-current so the breakdown voltage is determined by the recovery curve again. Therefore the recovery curve describes the 'cold' breakdown voltage of the VCB. From (12) and (13) the current interruption criterion can be stated as:

$$U_m < \alpha U_b \tag{14}$$

U_m can also be written as a function of i_l, the amplitude of the preceding HF-current:

$$U_m = f_p U_{c0} = f_p L_{hf} \left| \frac{di}{dt} \right|_{cz} = f_p Z_0 i_l \tag{15}$$

where $|di/dt|_{cz}$ is the absolute value of di/dt at the moment of current zero and

$$Z_0 = \sqrt{\frac{L_{hf}}{C_{hf}}} \tag{16}$$

The breakdown voltage reduction factor α is a relative parameter and expected to be better suited to describe the HF-current interruption capability for a VCB than the maximum interruptable di/dt. This will be discussed in 5.3. The relation between α and i_l is investigated experimentally in chapter 3.

If we consider a current independent breakdown voltage reduction factor: $\alpha = \alpha_0$, something more can be said about the HF-arcing duration. From (10) and (11) it follows that:

$$U_m = f_p U_{bd} \exp\left(-\frac{nT}{2\tau}\right) \tag{17}$$

The exp-term can be written as:

$$\frac{nT}{2\tau} = \frac{n\pi}{\omega\tau} = \frac{n\pi R_{hf}}{2Z_0} = \frac{n\pi}{2Q} \tag{18}$$

with

$$\omega = \frac{1}{\sqrt{C_{hf}L_{hf}}} \; ; \quad \tau = \frac{2L_{hf}}{R_{hf}} \quad and \quad Q = \frac{Z_0}{R_{hf}} \tag{19}$$

When the interruption criterion is met: $U_m = \alpha_0 U_b$ it follows from (17) and (18):

$$f_p U_{bd} \exp\left(-\frac{n\pi}{2Q}\right) = \alpha_0 U_b \tag{20}$$

During one HF-arcing period U_b is only slightly changing: $U_b \approx U_{bd}$, so n can be written as:

$$n = \frac{2Q}{\pi} \ln\left(\frac{f_p}{\alpha_0}\right) \tag{21}$$

from which it can be seen that the number of half HF-current periods is a circuit constant (Q, f_p) which is only slightly dependent on α_0. The duration of the HF-arcing period is:

$$\Delta T = \frac{n\pi}{\omega} = \tau \ln\left(\frac{f_p}{\alpha_0}\right) \tag{22}$$

3. EXPERIMENTS

3.1 The synthetic circuit

As mentioned before, the aim of the research described in this report is to measure the interrupter parameters which determine the high frequency reignition behaviour for a medium voltage (7.2kV) type of VCB with six different contact materials: Cu, CuCr, AgWC, CuW, CuBi and CuTeSe. The behaviour during the described HF-phenomena has to be measured without the use of a complete inductive circuit, because of the high costs involved. Therefore a synthetic circuit was used, in which the same phenomena can be simulated. In figure 9 the synthetic circuit used is plotted.

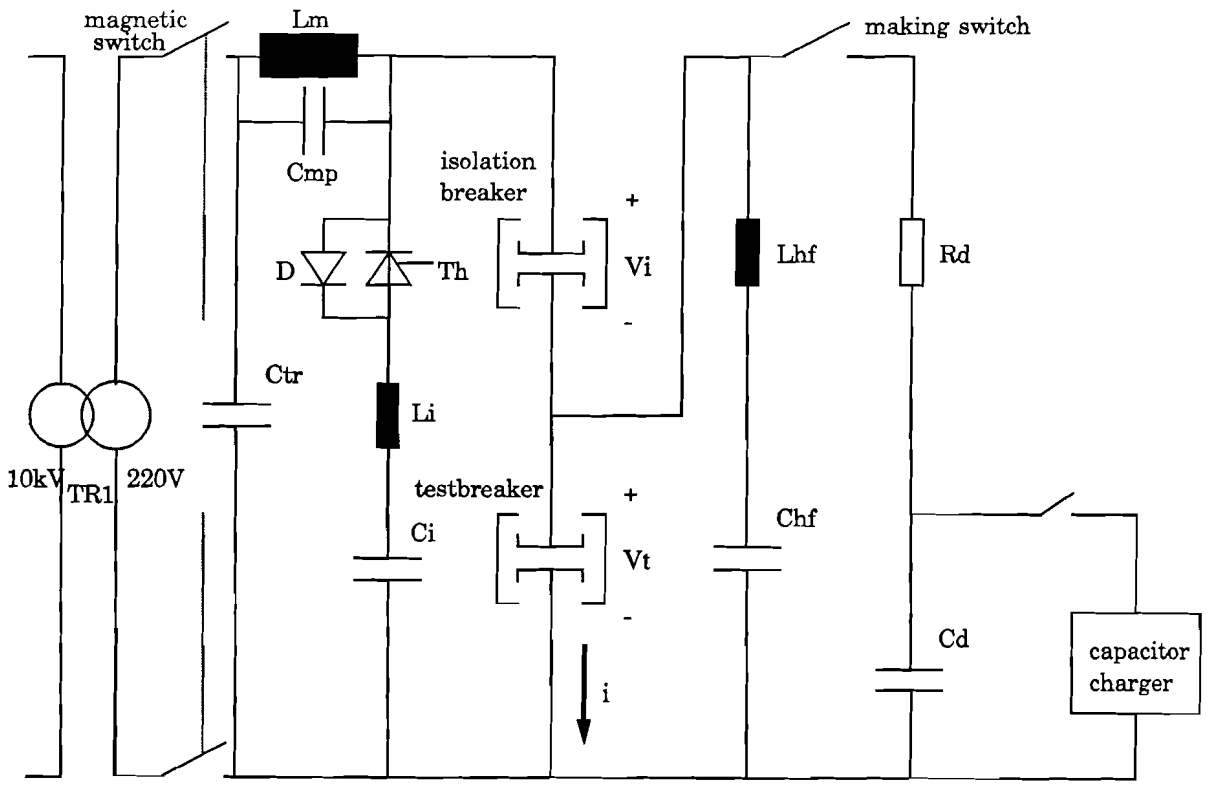

figure 9: synthetic circuit

The value of the components is:

L_m	17mH	C_i	1μF
L_{hf}	24μH	C_{hf}	5nF
L_i	1.5μH (parasitic)	C_d	111μF
		C_{mp}	60μF
R_d	5.6kΩ	C_{tr}	1μF

The circuit consists mainly of two parts, the low voltage (LV) part and the medium voltage (MV) part. The function of the former is to simulate the load current through the interrupter (see 'i' in figure 4). The latter simulates the TRV after current interruption (see 'U_{AB}' in figure 4 and LF/UHF-TRV in figure 6).

The two parts are formed by:

LV:
- 800kVA distribution transformer 10kV/220V providing a 50 Hz load current
- L_m, limiting the load current to about 50A peak value
- two VCBs: the test breaker and an auxiliary breaker (CuCr isolation breaker)
- C_{tr} and C_{mp}, limiting overvoltages at the transformer connections
- a current injection circuit formed by a thyristor (Th), an antiparallel diode (D), the injection capacitor C_i and a parasitic inductance L_i

The two VCBs are mounted in the same mechanism. When the command for opening the interrupters is given, the construction provides a mechanical delay of about 1ms between the isolation breaker and the test breaker, where the isolation breaker opens first. This function will be illustrated in 3.2. The injection circuit is used to create an artificial current zero, which will also be explained in 3.2. The diode allows a reversed injection current.

MV:
- the test breaker
- the bounce free making switch
- R_d and the capacitor bank C_d to provide the TRV
- the HF-circuit formed by C_{hf} and L_{hf}
- the capacitor charger 100mA 0-20kV (external power supply)

The HF-circuit provides the HF-current during a reignition (see figure 6 on page 9).

The voltage over and the current through the test breaker are measured by a high voltage 75MHz probe (1000:1) and a 20MHz current transformer (50mV/A) respectively, and the signals are registrated on a 2 channel 125MHz digital oscilloscope. The high voltage probe has been carefully calibrated by using a function generator (500V, risetime $\approx$ 20ns) and using the prebreakdown of the making switch with C_d charged to 5kV and the test breaker closed, resulting in a very steep voltage decay (approx. 110kV/μs). In 3.3 problems with the high voltage probe measurement are discussed. Various other voltages are measured for control. For more details on equipment used, see appendix A on page 46. The whole process is controlled by a timer unit based on a 8085 microprocessor. Before starting the measurements each interrupter was conditioned with a 30A DC current. For both current directions a charge of 50C has been applied.

3.2 The measuring process

The process starts with both VCBs closed. The 50Hz load current of about 50A peak value is switched in by the magnetic switch and is limited by L_m. After about 100ms the inrush phenomenon is damped out and the 50Hz current has become symmetric. After that, both VCBs are opened by the described mechanism approximately at the moment of negative current maximum. First there will be an arc in the isolation breaker. After the mechanical delay of about 1ms there will be an arc in the test breaker. This can be seen in figure 10, where the voltage over the two breakers and the current through the breakers is plotted. The two arc voltage steps of about 17V each cause a current oscillation of 4.3kHz caused by L_m and C_{mp}. It can be seen from figure 10 that C_{mp} should not be too large in order to avoid an undesirable current zero.

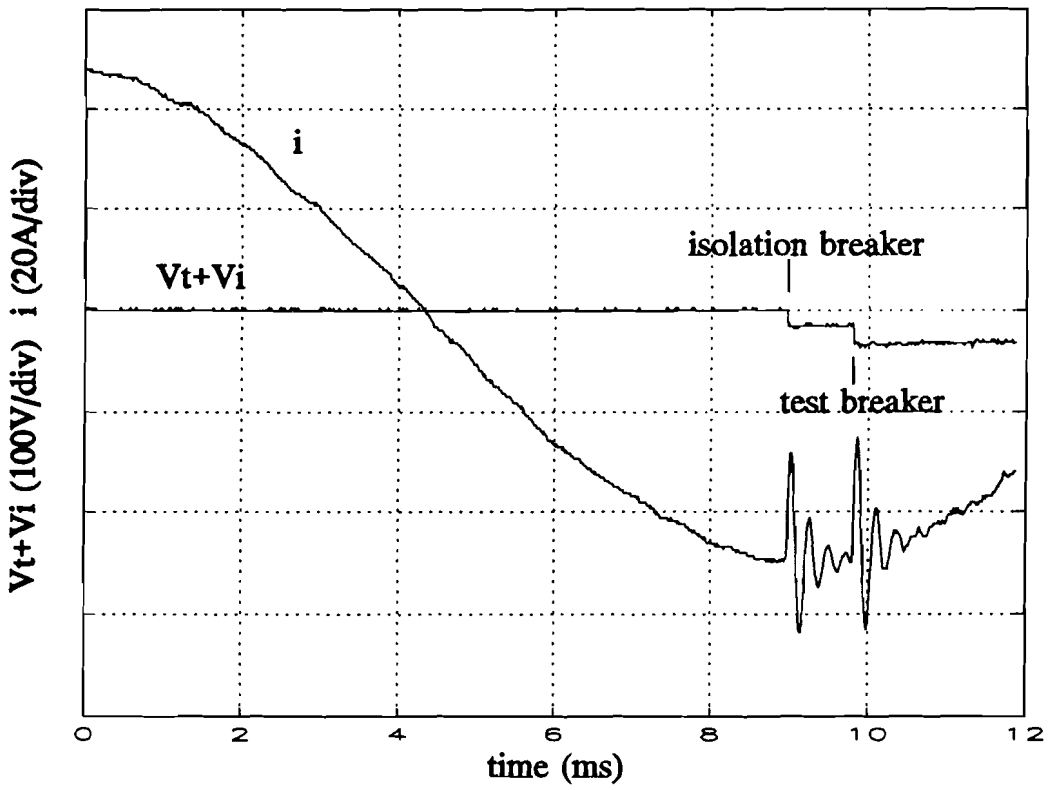

figure 10: measurement of the two arc voltages and the load current

When the test breaker starts to open, the current is still at its maximum. As mentioned before, HF-reignitions appear for very small gaps at the moment of current zero, which means for example an arcing time of 30μs. Therefore, the current injection circuit is used to create an artificial current zero by injecting a current opposite to the momentary load current direction. The injected current varies from 130kHz 180A to 12kHz 33A by changing L_i and C_i. The reason for not using the 'natural' 50Hz current zero is the difficulty of timing: it is impossible to open the interrupter mechanism with a 10μs precision before current zero. So the procedure is as follows:

- detect the second arc voltage (which means the test breaker opens)
- wait for 30μs
- trigger the thyristor: an artificial current zero appears

After the current zero, the TRV has to be applied. Therefore C_d is charged to 15kV. The making switch is closed a few ms before the opening of the test breaker so there will be no voltage drop of C_d, because the RC-time R_dC_d is 0.62s. The closing of the making switch results in a rising TRV at the moment of current zero, which causes the desired HF-reignitions. This TRV has a '1-exp' shape caused by R_d and C_{hf} (since $C_{hf} \ll C_d$). The time constant is 28μs. The process with current injection and TRV can be seen in figure 11, where the voltage over and the current through the test breaker is plotted.

In figure 12 the HF-reignition series can be seen on a larger scale. Similar to figure 6 on page 9, the HF-current and the 'reignition spikes' can be seen in this measurement. The secondary transformer connections are protected against these 'spikes' by the fast dielectric recovery (CuCr) and the larger gap of the isolation breaker.

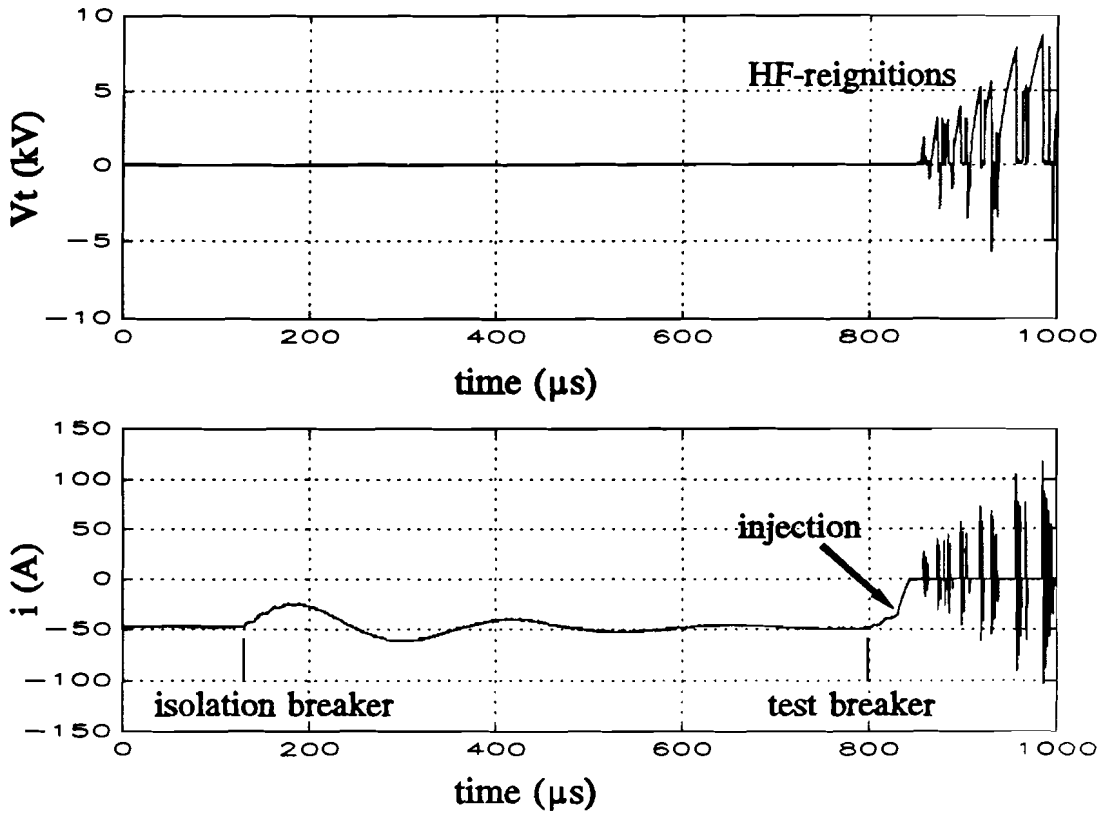

figure 11: opening of breakers followed by HF-reignitions

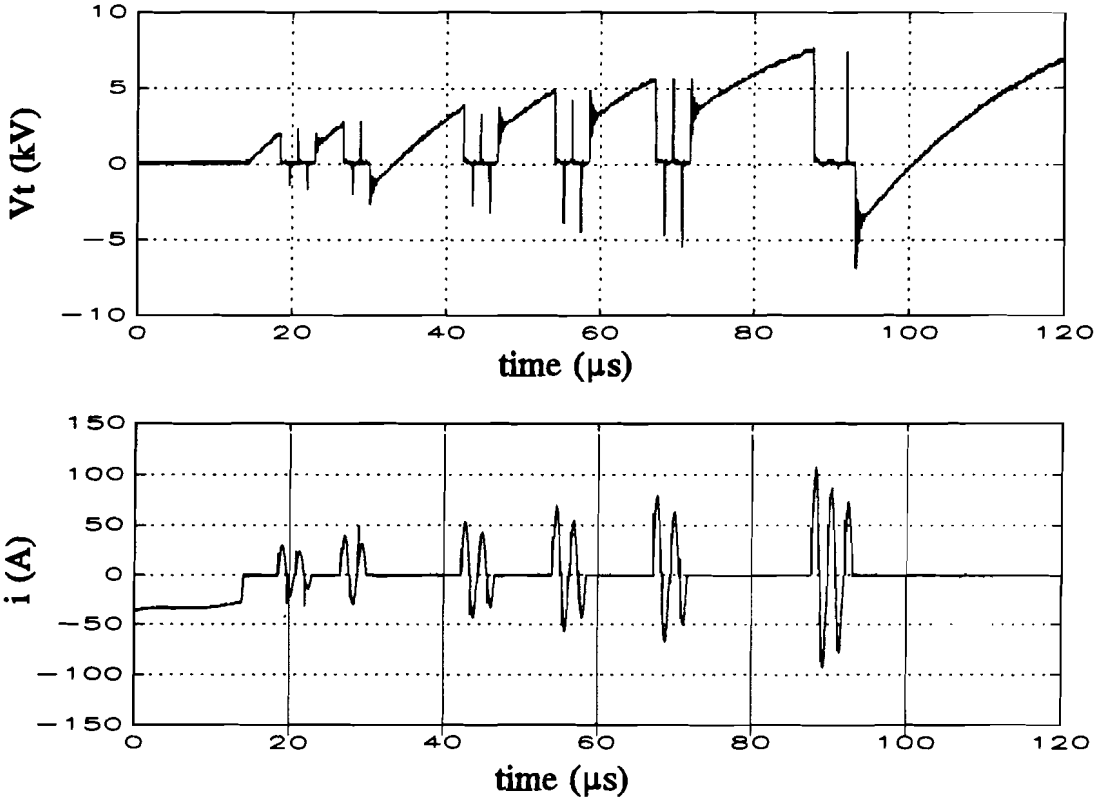

figure 12: HF-reignitions in test breaker

3.3 Voltage measurement problems

The HF-current in figure 12 has a frequency of 473kHz and an amplitude up to 180A. It is clear that this current causes a relatively strong HF magnetic field which causes interference with the measurement of the test breaker voltage V_t. This problem is illustrated in figure 13.

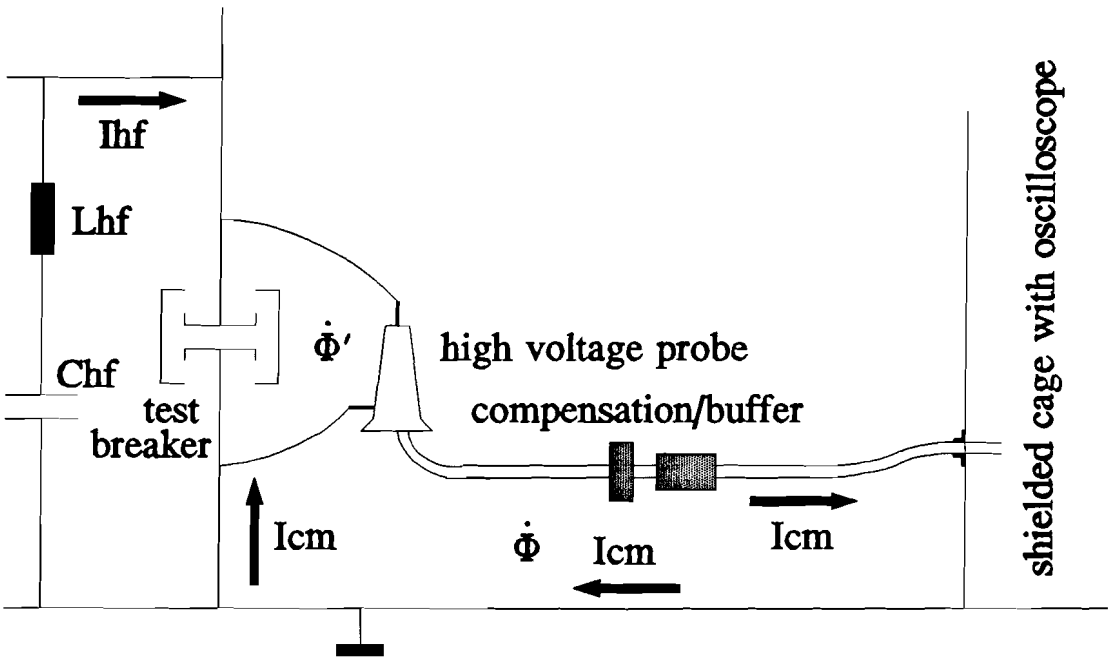

figure 13: interference by HF magnetic field

Because of the long distance (8m) from the high voltage probe to the oscilloscope, the compensation box of the probe is connected to a 50Ω coax cable by a buffer amplifier with an input impedance of 1MΩ and an attenuation ratio of 2. The coax cable shielding is connected to the shielded cage. The amplifier also has a connection to the supply voltage, which is not plotted. $d\Phi/dt$ represents the changing flux caused by the magnetic field in the loop formed by the high voltage probe earth connection, the compensation box, the buffer amplifier, the shielded cage and the lab ground. This $d\Phi/dt$ induces a current in the described loop, called 'common mode' current I_{cm} [6]. I_{cm} (order of 10A) is coupled into the measured signal in three ways:

- by the 'transfer impedance' Z_t of both coax cables which is defined as the extra signal voltage divided by I_{cm}. Z_t is strongly dependant on the quality of the coax cabel.

- by the compensation box and the buffer amplifier. I_{cm} causes an internal magnetic field inside these two boxes, which influences the measured signal. Especially the amplifier is sensitive because of the unpredictable effects of the magnetic field to the electronics inside.

- by the supply voltage connection.

The described interference by I_{cm} is very harmful because the distortion is relatively

large compared to the attenuated (1:2000) measured signal level.

There is also a HF magnetic field coupled into the unavoidable loop formed by the high voltage probe and the test breaker, $d\Phi'/dt$. The voltage induced in this loop is relatively small compared to the measured signal and causes no major distortion.

Two solutions were used:

- The buffer amplifier was removed, the compensation box was directly connected to the oscilloscope. Along the remaining distance to the test breaker a transmission line of 300Ω was used.

- The transfer impedance of the probe cable was reduced by using an additional copper shielding.

The solutions are illustrated in figure 14.

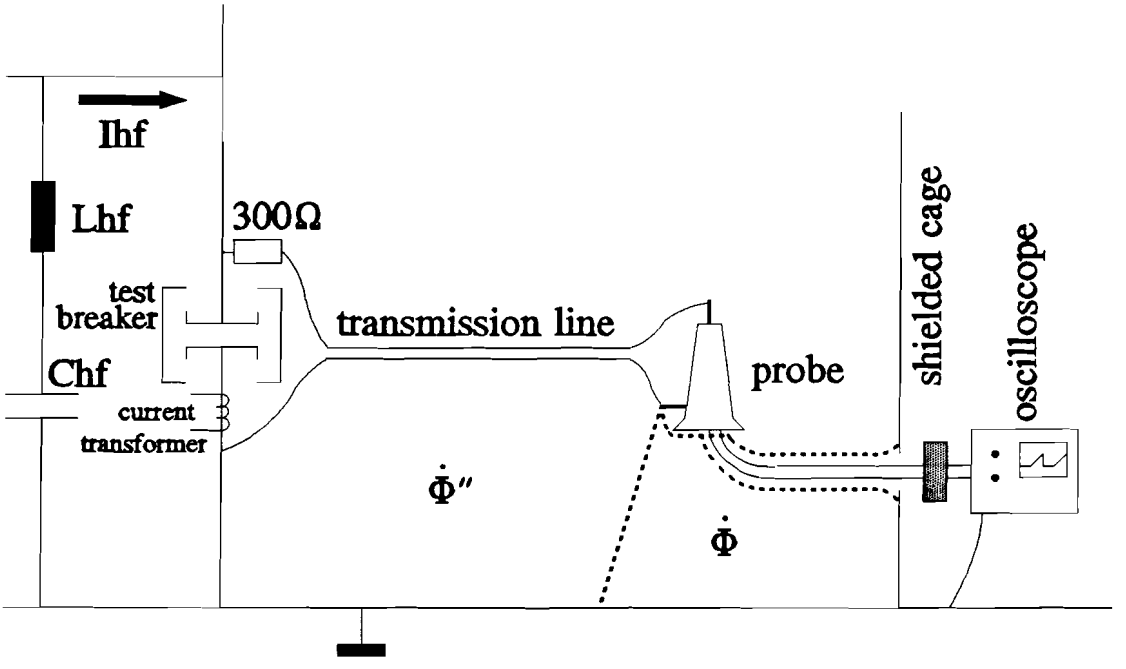

figure 14: improved voltage measurement

Because of the high input impedance of the high voltage probe (100MΩ, 3pF), the transmission line has a characteristic termination at the interrupter side.

The additional copper shielding is plotted with dashed lines. It is very well connected with the shielded cage, with the shielding of the coax cable at the probe side, with the earth connection of the probe and with the lab earth. In fact the copper shielding is an extension of the shielded cage. From the figure it is clear that the current induced by $d\Phi/dt$ flows through the copper shielding and <u>not</u> through the coax cable. I_{cm} in the coax cable is reduced below detection level so no distortion couples into the measured signal by way of the transfer impedance Z_t. The current in the loop enclosing $d\Phi''/dt$ also induces a voltage into the transmission line. This voltage is relatively small compared to the transmission line signal which is the unattenuated test breaker

voltage. So dΦ"/dt causes no major distortion.

The current transformer is placed between the transmission line connection and the VCB at the ground side, as indicated in figure 14. This is because now there is no distortion from the transmission line load current on the test breaker current measurement.

3.4 Definitions

In this report, a 'reignition' is defined as one half cycle of HF arcing. Four different types of reignitions can be distinguished according to the delay time (t_d) between the end of the previous reignition and the start of the actual reignition [7]:

type 1: This reignition starts after a relatively long time (delay > 5μs) after previous arcing at the 'cold' breakdown voltage U_b. In all cases, this is the first reignition of a series and considered to be a dielectric reignition. As mentioned before, it is assumed that for this type of reignition there will be no influence of the preceding HF-current

type 2: This reignition starts immediately (delay < 10ns) after the previous reignition at a low (< 800V) level of breakdown voltage. Therefore the breakdown voltage reduction factor is close to zero. It is considered to be a thermal reignition.

type 3: This reignition starts very short (20ns < delay <100ns) after the previous reignition at a high level (> 2kV) of breakdown voltage, therefore the breakdown voltage reduction factor is close to 1. It is also considered to be a dielectric reignition.

type 4: This reignition starts a relatively long time (200ns < delay < 3μs) after the previous reignition, at a moderate level of breakdown voltage. Essential for this type is that the maximum of UHF-TRV has occured prior to the (lower) voltage at which this reignition starts, thus it is no dielectric reignition. It is no thermal reignition either because at the moment of reignition there is a certain voltage across the gap. It is a delayed reignition for which the breakdown voltage reduction factor is not defined.

A 'measurement' is defined by one sequence of 50Hz arcing, followed by a number of series of reignitions. A 'series of reignitions' or 'series' is a group of reignitions that occurs closely (with a currentless time of less than 3μs) after each other. For example in figure 12 on page 17 one measurement with six series can be seen. Every series always starts with a type 1 reignition. An 'element' of the series is a group (containing one or more) of successive reignitions that starts with type 1, 3 or 4 (high breakdown voltage), and contains only one of these types. These definitions are illustrated in figure 15, where one measured series of reignitions in AgWC can be seen. The data were collected by registrating the following parameters, illustrated in figure 16:

type: the type (1, 3 or 4) of the first reignition in the element.
t_d: the time that has elapsed since the previous current zero.

t_b: the time (measured from contact separation) of start of the first reignition in the element.

U_b: the breakdown voltage (type 1) or reignition voltage (type 2, 3 and 4) at the start of the first reignition in the element.

i_l: the current amplitude of the last reignition in the element.

U_m: the maximum of the UHF-TRV that appears after current zero of the last reignition in the element (only when the next element start with type 1 or 4).

n: the number of reignitions in the elements. The number of type 2 reignitions in an element is always (n-1).

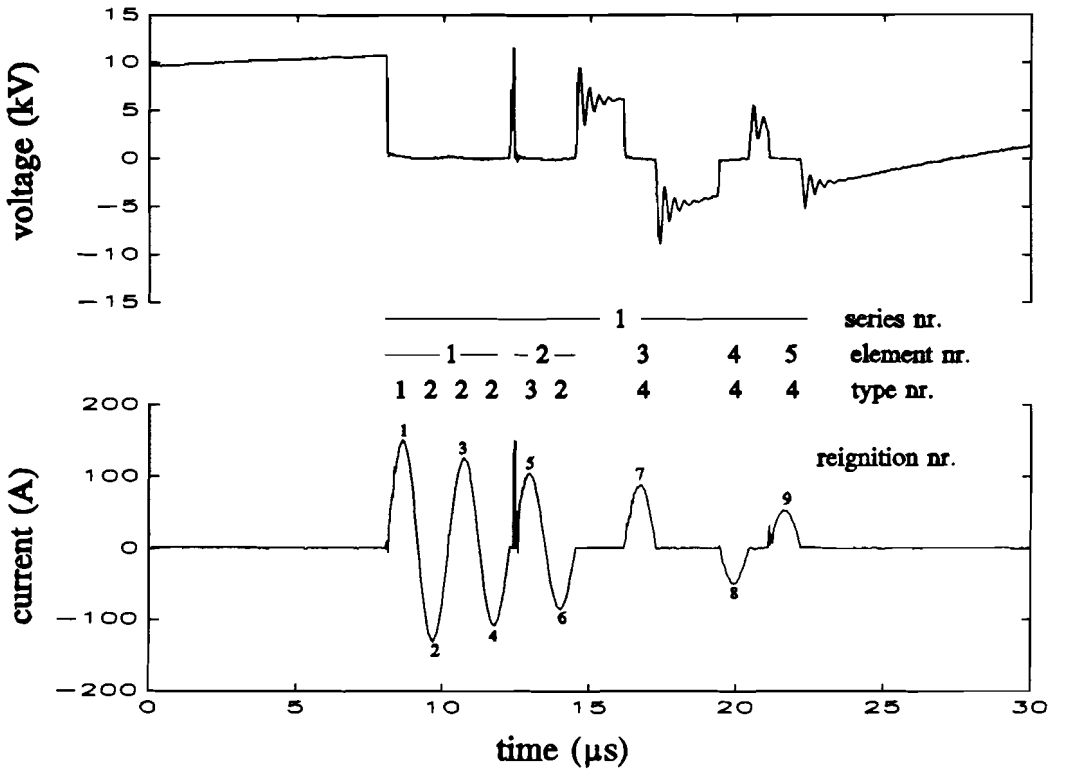

figure 15: definitions of reignition series, elements and types

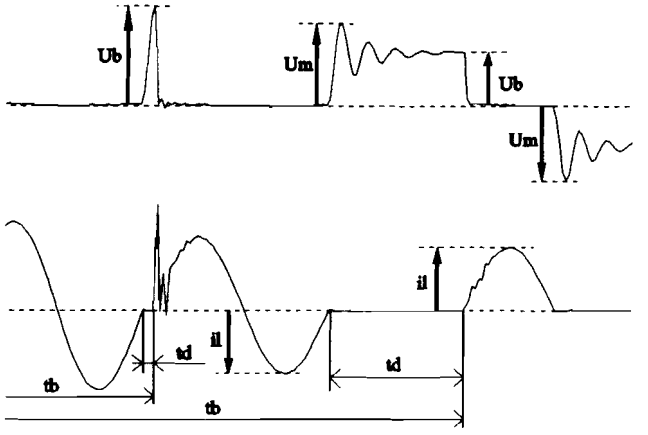

figure 16: the measurement parameters

The measurement data was entered into a database for further calculation.

4. RESULTS

For each contact material several measurements were done as shown below:

	Cu	CuCr	AgWC	CuW	CuBi	CuTeSe
# measurements	14	5	7	6	4	2
# series	65	52	71	49	77	76
# reignitions	228	258	476	464	435	301

4.1 The dielectric recovery

The cold breakdown voltage is determined by type 1, the dielectric reignitions after a currentless time of at least 5μs. The measurement results for the six different contact materials are plotted in figure 19 and figure 20. A large difference in dielectric recovery can be seen, while the opening speed was in the order of 1m/s to 1.5m/s. The opening speed was checked for the Cu and AgWC switch using a simple mechanism shown in figure 17.

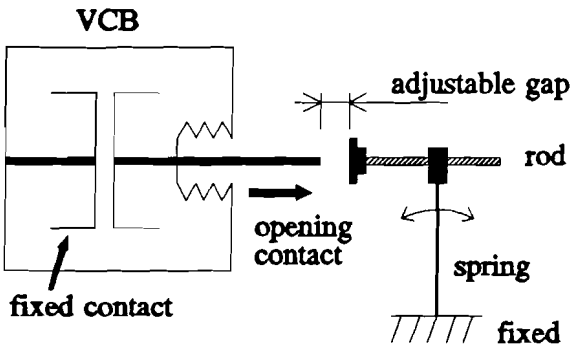

The adjustable gap can be changed from 0 to 3mm. For five different gap lengths the delay time was measured between the opening of the VCB and the closing of the speed measurement mechanism. The result is shown in figure 18. The number of measurements for each gap length is at least five.

figure 17: speed measurement mechanism

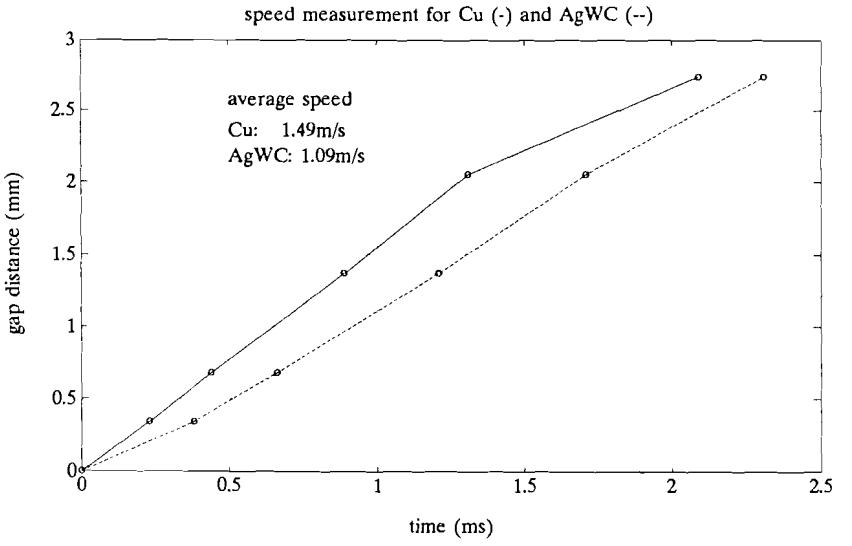

figure 18: result of speed measurement

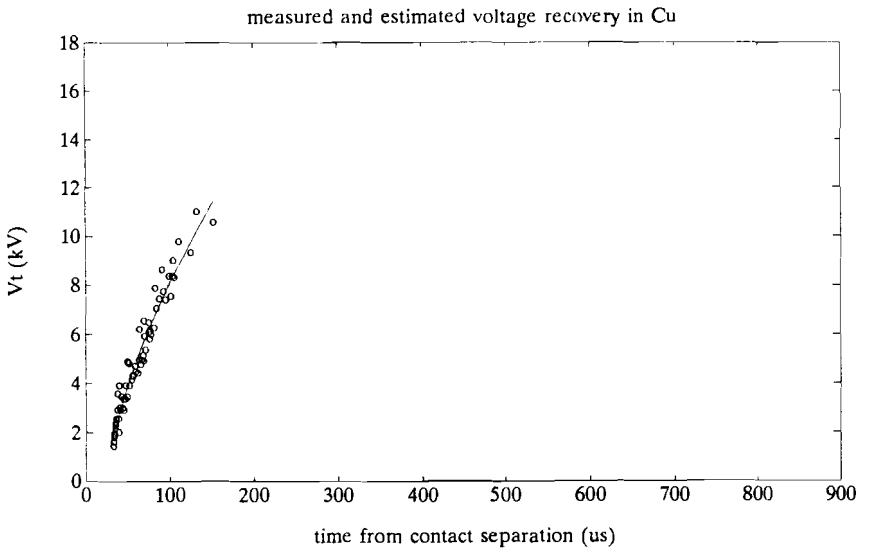

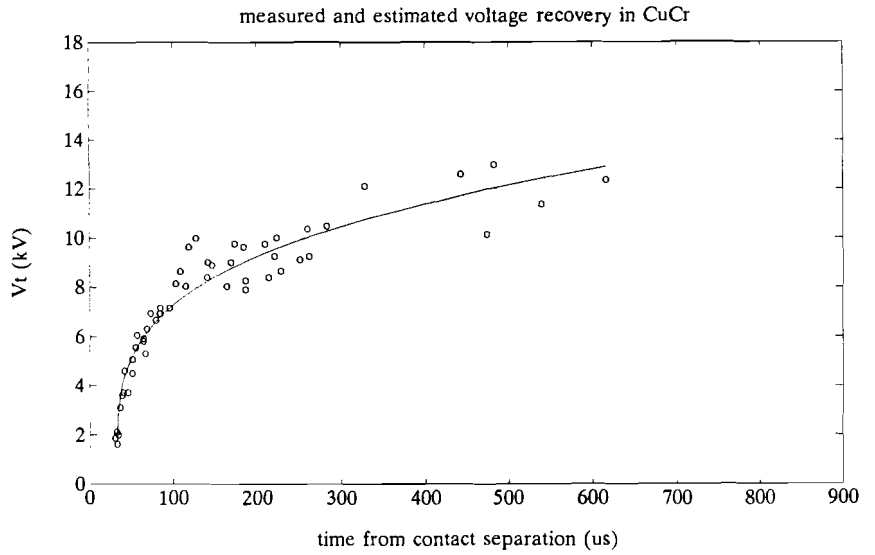

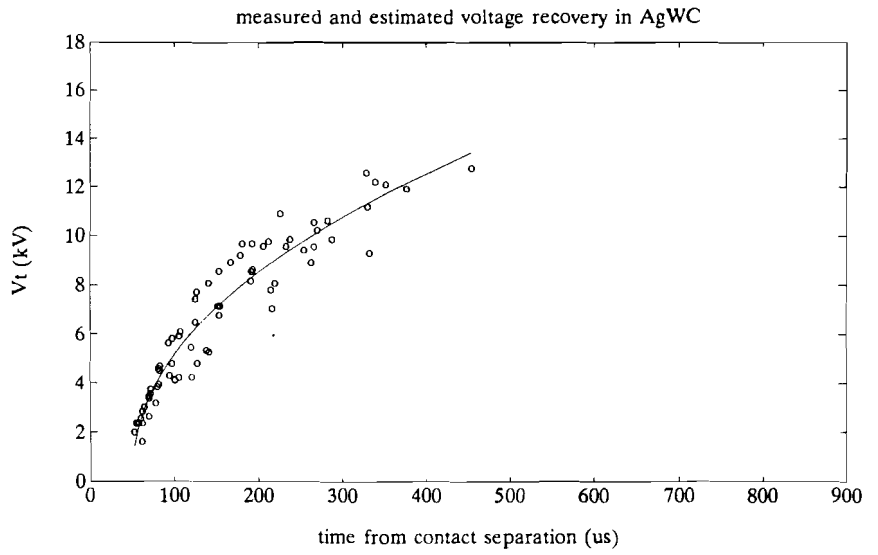

figure 19: dielectric recovery for Cu, CuCr and AgWC

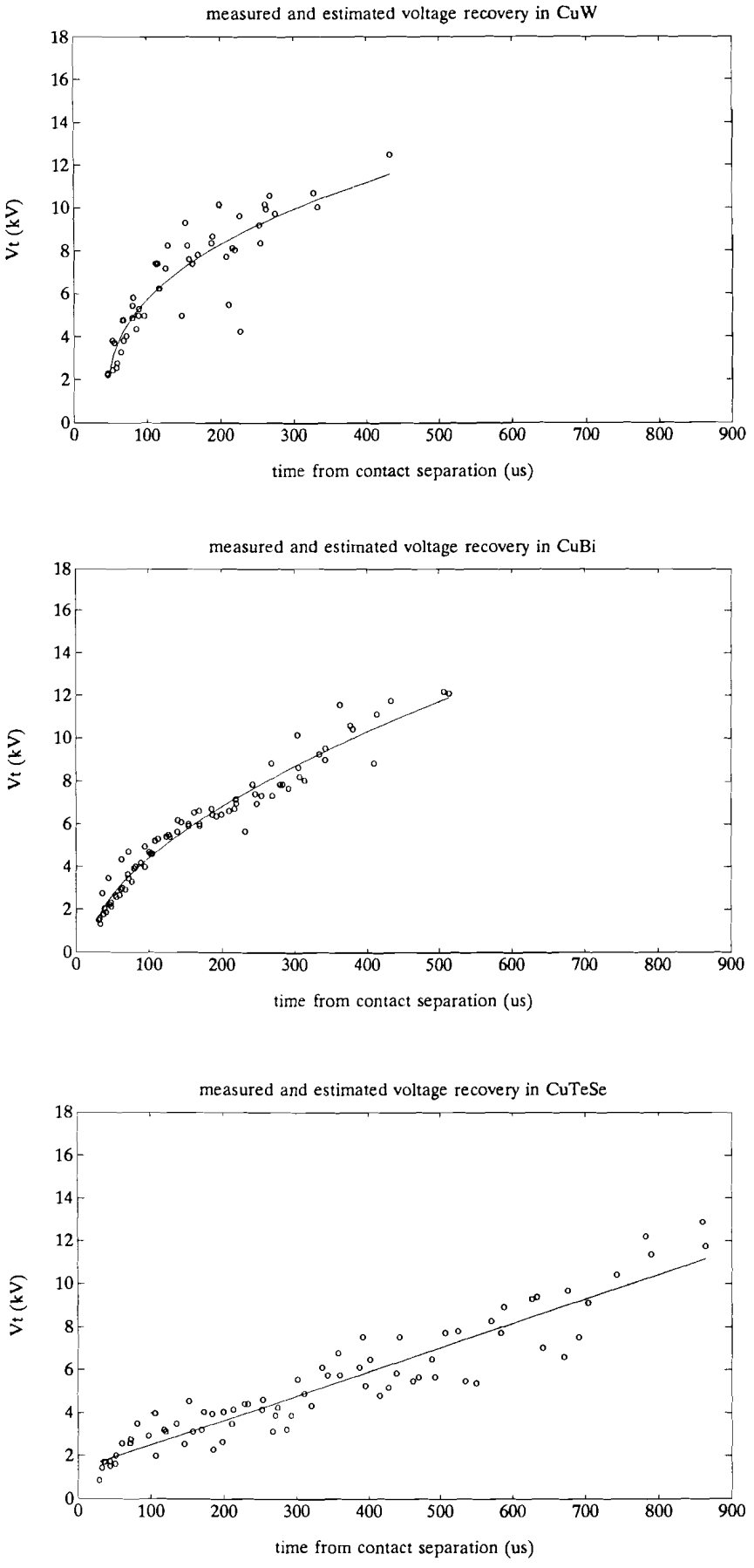

figure 20: dielectric recovery for CuW, CuBi and CuTeSe

In order to be able to calculate the breakdown voltage reduction factor at each current zero, the dielectric recovery has to be estimated by a function. Empirically it was found that the best estimation, except for CuTeSe, is given by:

$$U_b(t) = b \cdot (t_b - c)^d \tag{23}$$

where $U_b(t)$ is the dielectric recovery and t_b is the time measured from contact separation. The constant c is introduced because the dielectric recovery starts 30μs-50μs after contact separation, at the moment of the artificial current zero. The constants b, c and d are found for each contact material using a least squares method algorithm. Only the dielectric recovery of CuTeSe could be described by a straight line:

$$U_b(t) = b \cdot t_b + c \tag{24}$$

The estimated curves are plotted also in figure 19 and figure 20. The calculated parameters are shown in the following table.

	Cu	CuCr	AgWC	CuW	CuBi	CuTeSe
b	443	2369	854	1309	370	11.3
c	24.6	31.7	49.4	42.8	16.2	1355
d	0.67	0.27	0.46	0.37	0.56	-

4.2 Reignition types

In a serie each type 1 reignition is followed by one or more type 2, type 3 or type 4 reignitions. The relative appearance of these types can be seen in figure 21 for each contact material. From this it can be concluded that about 90% of the reignitions in Cu and CuCr is dielectric, while for AgWC, CuW, CuBi and CuTeSe 26% to 45% is dielectric and 48% to 66% is thermal. Delayed reignitions only occur in CuCr, AgWC, CuW and CuTeSe.

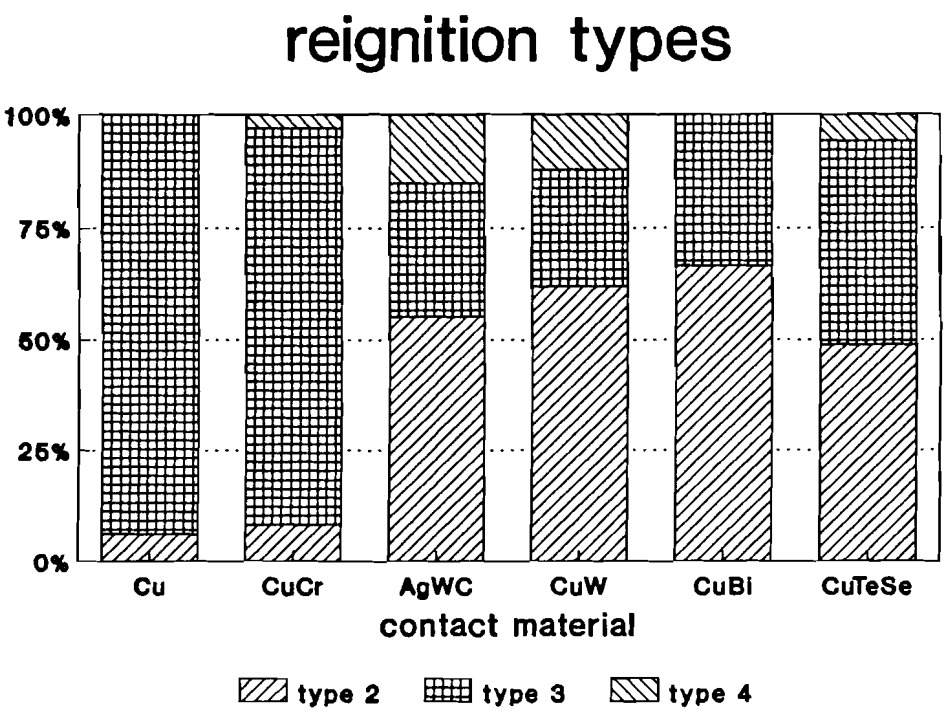

figure 21: relative appearance of type 2, 3 and 4

4.3 The high frequency interruption capability

It can be expected that the momentary breakdown voltage is reduced by the preceding arc activity. As outlined in 2.3, this is described by the breakdown voltage reduction factor α. Here, the dependence on current of α is reported.

In figure 22 and figure 23 the breakdown voltage reduction factor is plotted for the six contact materials as a function of i_l, the current amplitude preceding the HF-current zero. Each measured point in these plots is one type 2 or 3 reignition. A type 2 reignition is plotted as $\alpha = 0$.

In order to study the influence of the 50Hz current on the HF-reignitions the percentage of reignitions (type 2 or 3) for positive and negative i_l is presented in the following table:

percentage of reignitions	$i_l > 0$	$i_l < 0$
Cu	61%	39%
CuCr	58%	43%
AgWC	56%	44%
CuW	58%	42%
CuBi	58%	42%
CuTeSe	57%	43%

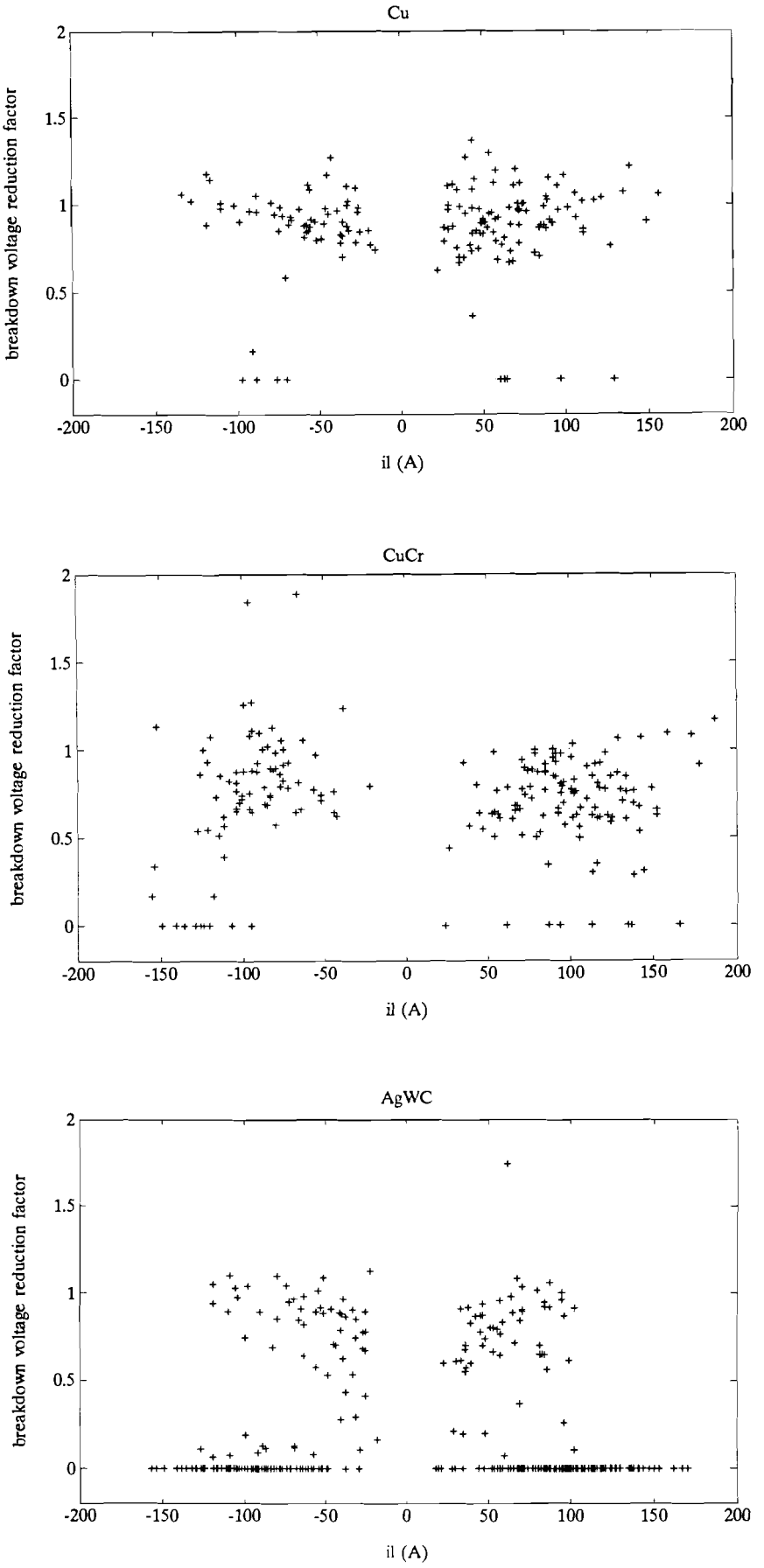

figure 22: breakdown voltage reduction factor for Cu, CuCr and AgWC

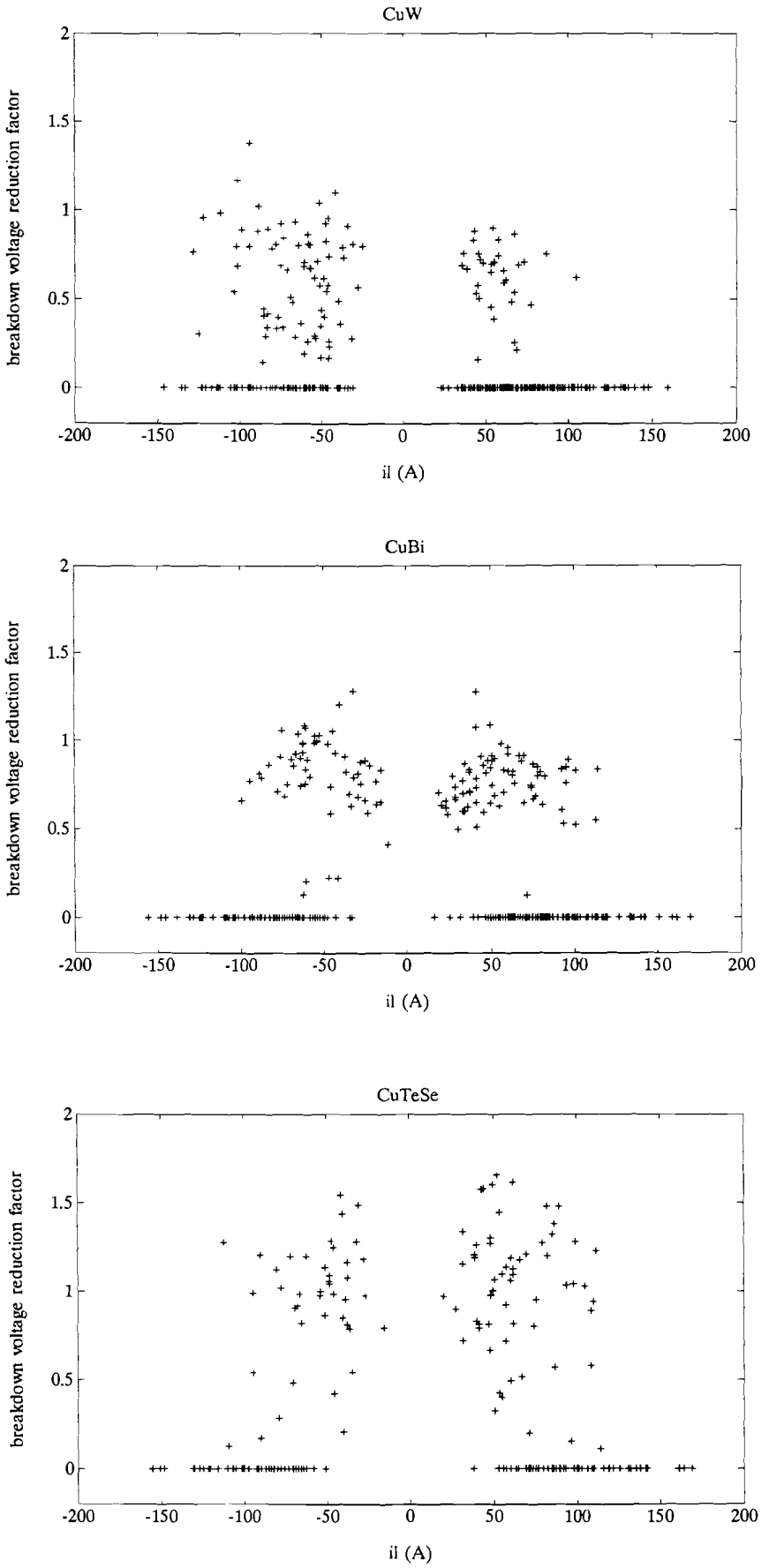

figure 23: breakdown voltage reduction factor for CuW, CuBi and CuTeSe

From the table it can be seen that for all contact materials there are more reignitions when the HF-current has been positive ($i_l > 0$). This can be explained in two ways:

- The HF-current always starts with a positive half sine, because the breakdown voltage for type 1 is always positive (see figure 12 on page 17). Therefore the number of positive half sines can be larger than the number of negative half sines. For CuTeSe it was found that only 21 of the 76 series have one reignition in total, for the other contact materials all series have two or more reignitions. So it can be concluded that this effect is negligible.

- The 50Hz current preceding the HF-reignitions is always negative (see figure 11 on page 17), so cathode spots are formed on the contact indicated with '+' in figure 9 on page 14. This means that most energy has been dissipated on this contact. This means that a reignition will be easier for a negative UHF-TRV, after which the HF-current will flow in the same (negative) direction as the 50Hz current. A negative TRV appears after a positive i_l (see figure 6 on page 9), so the result meets the expectation.

The 50Hz current in the synthetic circuit is a worst case compared to the situation in a real network, because the di/dt preceding a 'natural' 50Hz current zero is smaller than the di/dt preceding the current injection (see figure 10 and figure 11). So in a realistic circuit not much influence of the current polarity is expected. From figure 22 and figure 23 it can also be seen that the magnitude of the reduction factor is not influenced by the current polarity. So no more attention will be paid to the polarity effect.

Only for Cu it can be clearly seen that there is no tendency as a function of i_l and that all points are close to a constant average. To be able to draw conclusions for the other contact materials, an average value of the reduction factor is calculated for each current interval of 20A with at least 4 data points. The result can be seen in figure 24 where the average reduction factor is plotted as a function of the absolute i_l. For added clarity the calculated averages are connected by an estimated curve for each contact material.

For AgWC, CuW, CuBi and CuTeSe the reduction factor is low for larger i_l, for Cu the reduction factor does not show a clear tendency, for CuCr there is a small reduction for the higher values of i_l. The question is whether the reduction for larger i_l is caused by a reduction of the reignition voltage relative to the 'cold' breakdown voltage or by a relative increase of the number of thermal reignitions (type 2; $a=0$). To investigate this, in figure 25 the result is plotted only for type 3.

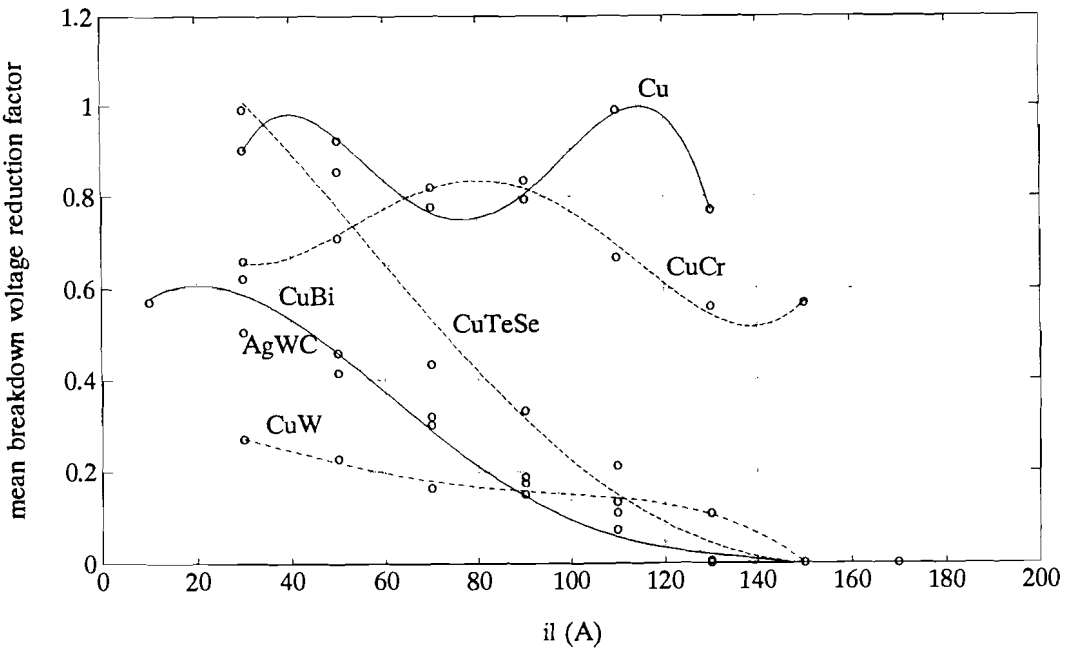

figure 24: mean breakdown voltage reduction factor for type 2 and 3

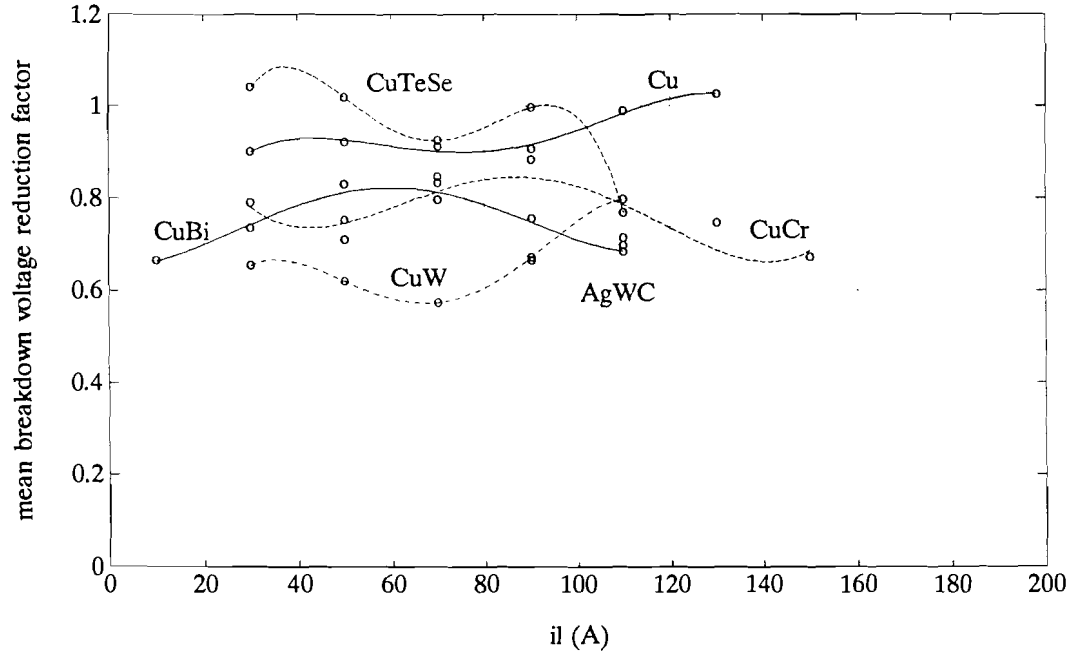

figure 25: mean breakdown voltage reduction factor for type 3

From figure 25 it can be seen that for all contact materials, the reduction factor does not show a clear tendency as a function of i_l, so the reduction of the reduction factor is caused by the increase of thermal (type 2) reignitions at higher currents.

This can be seen from figure 26 where the percentage of type 2 reignitions as a function of i_l is plotted.

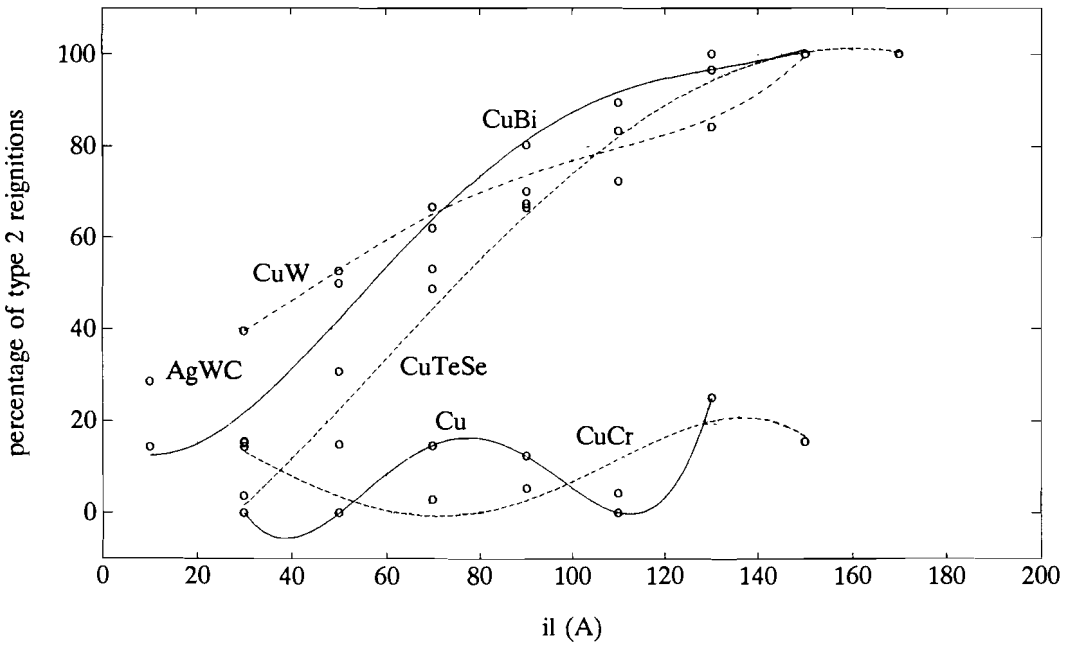

figure 26: percentage of type 2 reignitions

The percentage of type 2 reignitions increases up to 100% for AgWC, CuW, CuBi and CuTeSe, while the percentage of type 2 reignitions for Cu and CuCr stays low.

The breakdown voltage reduction factor is not defined for type 4 reignitions, though it is useful to know when a delayed reignition (type 4) will appear. It is not clear what phenomenon causes a type 4 reignition. In spite of that a relation between the percentage of type 4 reignitions and the preceding current has been found and can be seen in figure 27.

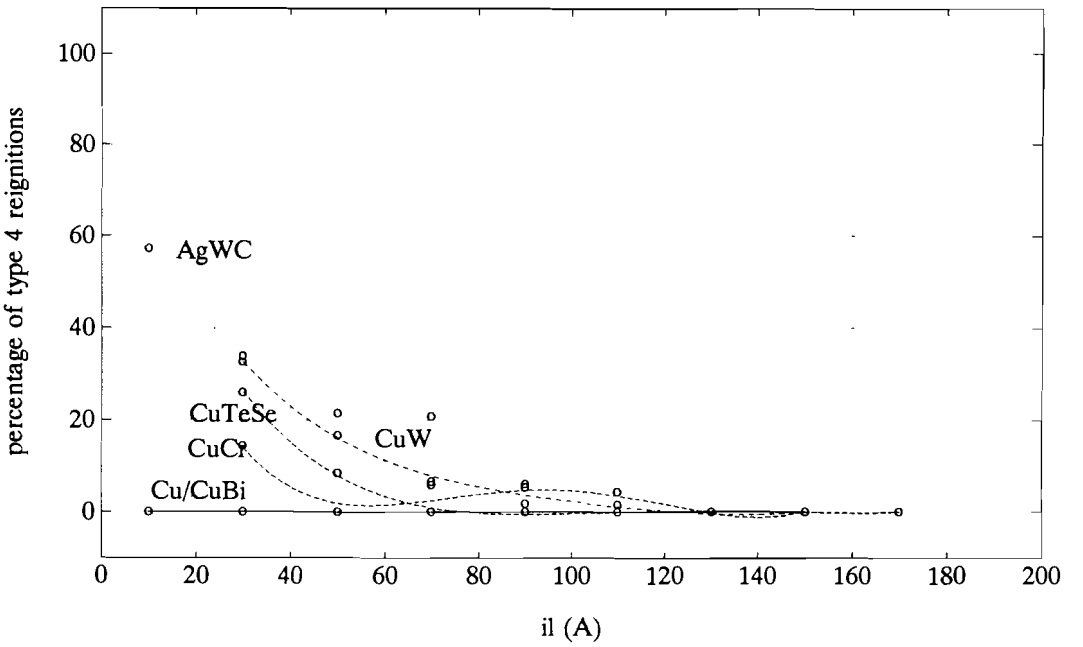

figure 27: percentage of type 4 reignitions

5. MODELLING

As mentioned before, the aim is to identify criteria for HF-current interruption for use in simulation programs. As mentioned in 2.2.3 for simulation it is necessary to know when a reignition will appear (dielectric recovery) and when the following HF-current will be interrupted (HF-current interruption capability) [2], [3]. In other words, the duration of the HF-current is important. This is because in real circuits, power frequency current is charging the inductive load during the period of HF arcing, thus increasing the stored energy in the load.

The dielectric recovery can be described by the parameters found in 4.1. The results presented in chapter 4 are used to create a model of the HF-current interruption capability which will be discussed in this chapter.

5.1 The high frequency current interruption capability

As shown in figure 25 on page 30 the breakdown voltage reduction factor for dielectric reignitions (type 3) can be defined as a constant α_0. So for type 3 the criterion for HF-current interruption as given in (14) can be stated as:

$$U_m < \alpha_0 U_b \tag{25}$$

where U_b is the well known dielectric recovery as given in (23) and (24). For each contact material α_0 is the average of the breakdown voltage reduction factor for type 3.

From figure 26 on page 31 it can be seen that the number of thermal (type 2) reignitions increases for a higher preceding HF-current amplitude. In order to describe this phenomenon in the model, an equivalent thermal reduction current i_{th} can be defined. i_{th} is the current amplitude for which 50% of the reignitions is thermal. Together with α_0, i_{th} (which follows from figure 26) is given below:

	Cu	CuCr	AgWC	CuW	CuBi	CuTeSe
α_0	0.92	0.79	0.72	0.63	0.78	1.07
i_{th} (A)	>130	>150	72	46	57	76

For type 4 reignitions, it can be seen from figure 21 on page 26 that it forms a relatively small part of the reignitions. From the total number of reignitions the percentage of type 4 reignitions which are actually the last reignition in a serie and thus determining the HF-current interruption is shown below:

	Cu	CuCr	AgWC	CuW	CuBi	CuTeSe
percentage of type 4 as last reignition in serie	0%	0.4%	7%	6%	0%	0.3%

From this it can be concluded that the type 4 reignitions only have a small influence

on the HF-current interruption. The error introduced in the restored load current by one reignition skipped is ½T (T = HF-current period) times the 50Hz current di/dt: ½T·2π·50Hz·100A ≈ 33mA. Therefore, leaving type 4 out of the model will not introduce large errors.

5.2 The HF-current interruption model

The thermal and dielectric reignition behaviour have to be integrated in one model. Therefore the HF interrupting behaviour should be described by an effective value of the breakdown voltage reduction factor that includes:

- thermal (type 2) reignitions
- current dependence of the probability of thermal reignitions
- dielectric reignitions that are independent of prior current

It is assumed that if the current exceeds i_{th}, there is always a thermal reignition and when the current is smaller than i_{th}, there will be no thermal reignition. A simple description of the relevant phenomena can then be given by the following equation (13):

$$\begin{aligned} \alpha &= \alpha_0 \qquad i_l < i_{th} \\ \alpha &= 0 \qquad i_l > i_{th} \end{aligned} \tag{26}$$

The reignition voltage U_r can now be written as:

$$\begin{aligned} U_r &= \alpha_0 U_b \qquad i_l < i_{th} \\ U_r &= 0 \qquad i_l > i_{th} \end{aligned} \tag{27}$$

Together with the interruption criterion (12):

$$U_m < U_r \tag{28}$$

this is integrated in the model, which is shown in figure 28. The HF-current amplitude preceding a current zero is plotted on the horizontal axis (indicated with triangles). The prospective value of U_m following from (15):

$$U_m = f_p Z_0 i_l \tag{29}$$

is also plotted for each current zero.

The situation is plotted for a breakdown of the gap at a voltage U_b = 10kV. The reignition voltage U_r from (27) is plotted for α_0 = 0.8 and i_{th} = 80A. The HF-current starts with 130A, indicated with '1'. As long as the interruption criterion (28) is not met, in other words if $U_m > U_r$, there will be a reignition. The first six reignitions ('1' to '6') are thermal, because $i_l > i_{th}$. They are followed by two dielectric reignitions ('7' and '8'). The last reignition for this case ('8') is indicated with an arrow indicating the point where the interruption criterion (28) is about to be met. So for this case, the existence of 6 thermal reignitions has no influence on the HF arcing duration.

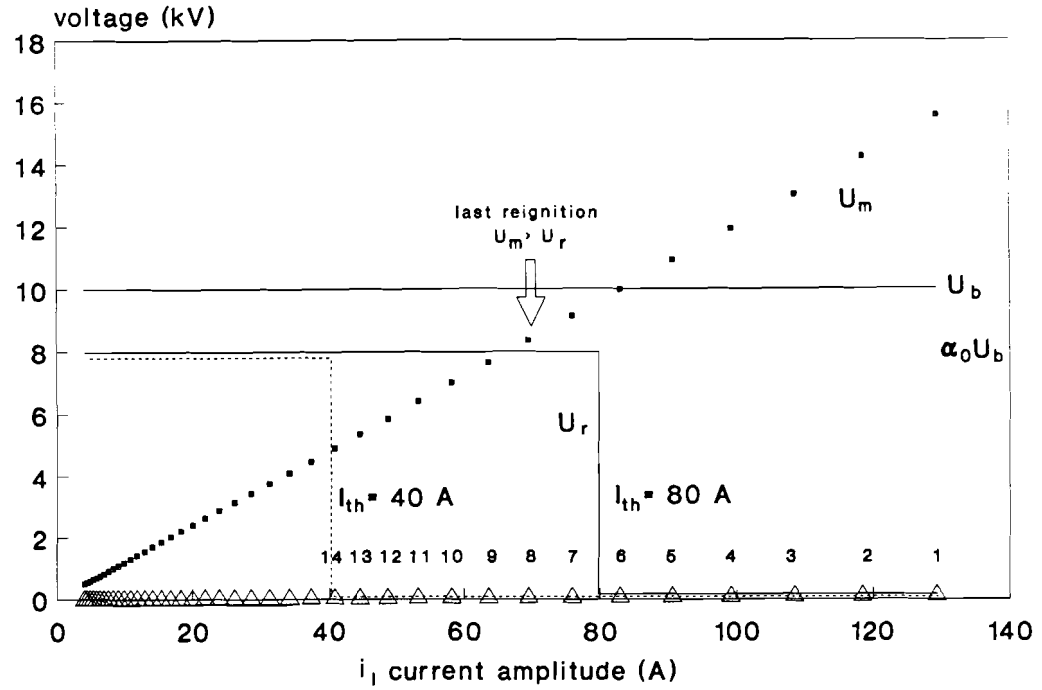

figure 28: the simulation model

The situation with a lower value of i_{th} (40A, U_r indicated with a dotted line) is plotted too. It can be seen that all reignitions ('1' to '14') are thermal because $i_l > i_{th}$. After the 14th reignition the interruption criterion (28) is met, so no dielectric reignitions follow. It is clear that in the latter case the overall duration of the HF arcing period is longer than in the case of i_{th} = 80A.

From the above, two regimes can be identified:

- Dielectrically dominated: thermal reignitions can go before dielectric reignitions, which appear at the end of the HF-arcing. (example of i_{th}=80A in figure 28). Interruption criterion: $U_m < \alpha_0 U_b$; α can be considered as a constant.
- Thermally dominated: only thermal reignitions are present, allowing U_m to decrease below the value $\alpha_0 U_b$ because U_r is kept zero during the total HF arcing period (example of i_{th}=40A). Interruption criterion: $U_m < \alpha(i_l) U_b$; now the current dependence of the reduction factor should be taken into account.

The two regimes are illustrated in figure 29 and figure 30 respectively.

The HF-current through the VCB ('i', dotted line) and the voltage over C_{hf} ('u') are plotted. The value of u at the moment of HF-current zero is indicated with U_{c0}. Also U_m (= $f_p U_{c0}$) is indicated. The 'cold' breakdown voltage U_b and the thermal reduction current i_{th} are plotted as horizontal lines. The reignition voltage U_r is plotted as pointed out in (27).

In figure 29 there are thermal reignitions (U_r = 0) as long as $i > i_{th}$. It can be seen that if i becomes smaller than i_{th}, U_m is still larger than U_r. This means that dielectric reignitions follow (in this case two) until U_m has become smaller than U_r.

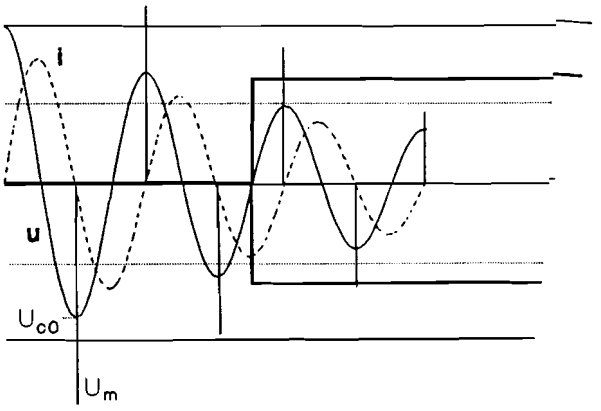

figure 29: dielectrically dominated HF-current interruption

In figure 30 it is clear that U_m has become smaller than U_r if $i < i_{th}$, so no more (dielectric) reignitions will follow.

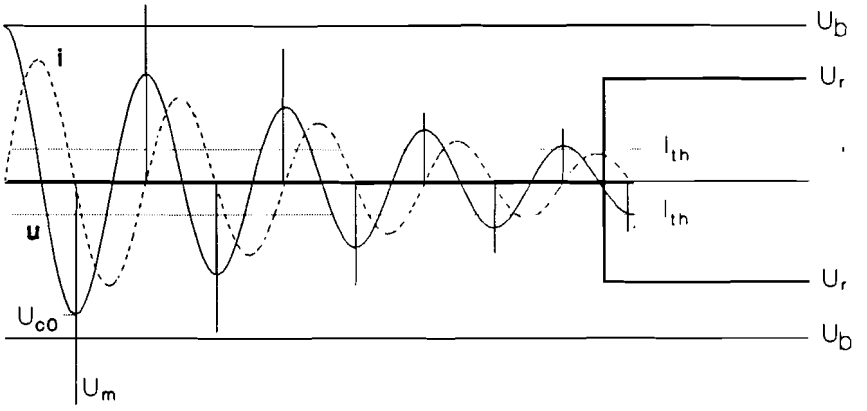

figure 30: thermally dominated HF-current interruption

An example of a measured dielectrically dominated serie can be seen in figure 31. A measured thermally dominated serie can be seen in figure 32.

From the simulation model in figure 28 it follows that the question whether interruption is either dielectrically or thermally dominated is determined by the momentary cold breakdown voltage U_b:

$$\begin{aligned} \alpha_0 U_b &< U_m(i_{th}) \;:\; \textit{dielectrically dominated} \\ \alpha_0 U_b &> U_m(i_{th}) \;:\; \textit{thermally dominated} \end{aligned} \tag{30}$$

where $U_m(i_{th})$ is U_m which corresponds with i_{th}. With (29) this can be written as:

$$\begin{aligned} U_b &< \frac{f_p Z_0}{\alpha_0} i_{th} \;:\; \textit{dielectrically dominated} \\ U_b &> \frac{f_p Z_0}{\alpha_0} i_{th} \;:\; \textit{thermally dominated} \end{aligned} \tag{31}$$

From figure 28, figure 29 and figure 30 it follows that the interruption criterion can be written as:

$$\begin{aligned} U_m &< \alpha_0 U_b \quad \textit{dielectrically dominated} \\ i_l &< i_{th} \quad \textit{thermally dominated} \end{aligned} \tag{32}$$

From (11) and (18) i_l can be written as:

$$i_l = \frac{U_{bd}}{Z_0} \exp\left(-\frac{n\pi}{2Q}\right) \tag{33}$$

Together with (32) it follows for thermally dominated reignitions:

$$n = \frac{2Q}{\pi} \ln\left(\frac{U_{bd}}{Z_0 i_{th}}\right) \tag{34}$$

which is only determined by the 'cold' breakdown U_{bd}, the circuit (Z_0) and the thermal parameter i_{th}. For dielectrically dominated reignitions, we already saw in (21) that:

$$n = \frac{2Q}{\pi} \ln\left(\frac{f_p}{\alpha_0}\right) \tag{35}$$

which is only determined by the circuit (Q, f_p) and the dielectric parameter α_0.

In the following table the relative number of reignitions for which the two situations of (31) are valid respectively is shown:

	Cu	CuCr	AgWC	CuW	CuBi	CuTeSe
thermally dominated	0%	0%	13%	52%	38%	33%
dielectrically dominated	100%	100%	87%	48%	62%	67%

From this it can be concluded that except for CuW, the largest number of reignitions is dielectrically dominated for the measurements done.

The model explained in figure 28 is also demonstrated by one measurement of CuBi, as shown in figure 33, where the value of the prospective UHF-TRV maximum U_m is plotted vs. the momentary reignition voltage $U_r = \alpha_0 U_b$.

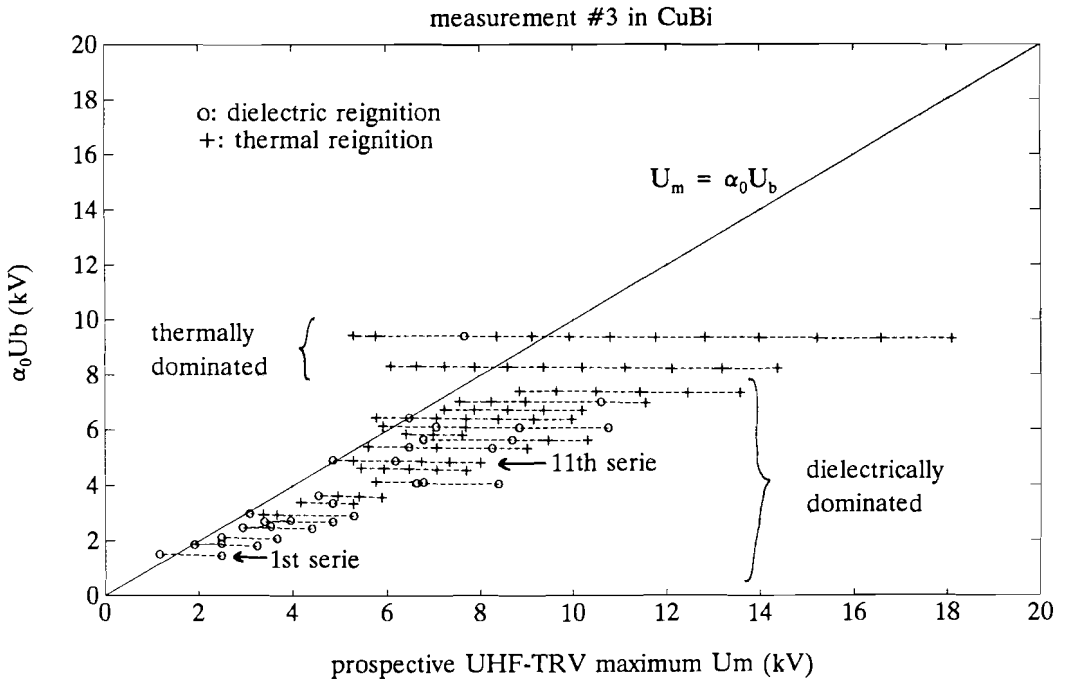

figure 33: third measurement of CuBi to demonstrate model

Each horizontal line is one serie of reignitions. The horizontal line in the lower left corner is the first serie (low value of $\alpha_0 U_b$). Each serie starts at the right side of the horizontal line (large HF-current: large U_m). The dielectric (type 3) reignitions are indicated by 'o', the thermal (type 2) reignitions are indicated by '+'. For the 11^{th} serie in figure 33 this is illustrated in figure 34.

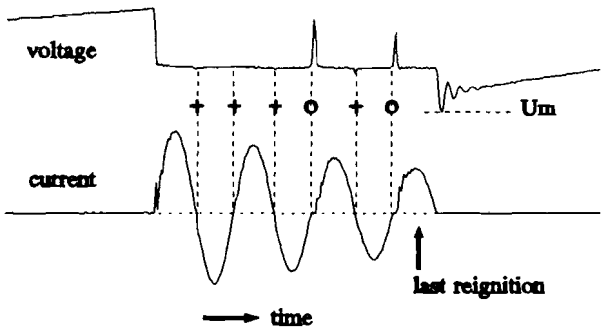

figure 34: 11th serie in third measurement of CuBi

From figure 33 it can be seen that the first series show most dielectric reignitions. For larger HF-currents, and thus larger U_m, the number of thermal reignitions increases. It is clear that in all series (except the last two) the HF-current stops when the interruption criterion $U_m < U_r$ is met, obviously these are dielectrically dominated. The last two series are thermally dominated.

In order to be able to show the phenomenon of figure 33 for each measurement, figure 35 is plotted. The average value of the momentary reignition voltage $U_r = \alpha_0 U_b$ is plotted vs. U_m for the last reignition in each serie. The idea is that at the last current zero of each serie of reignitions the interrupting criterion $U_m = U_r$ is met. This should be the case because for the measurements done, the largest number of reignitions is dielectrically dominated.

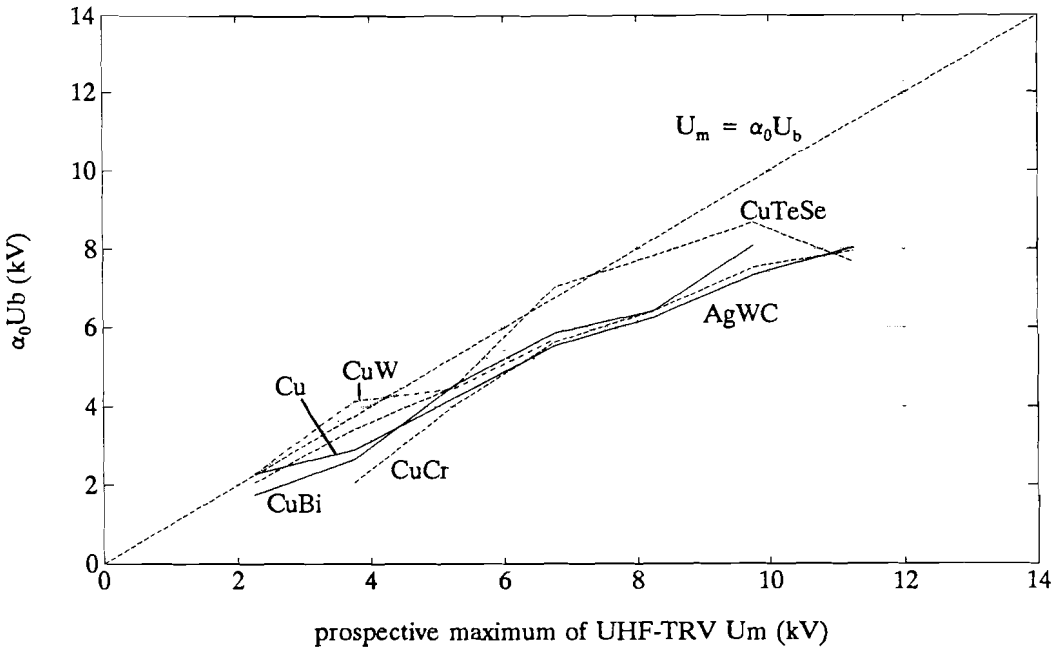

figure 35: U_m vs. reignition voltage $U_r = \alpha_0 U_b$

figure 35 proves that this is indeed the case, since the average value of the measured points are located very close to the line $U_m = U_r$. Only at higher reignition voltages the thermally dominated regime becomes important, resulting in a deviation from the

straight line towards the horizontal axis.

From figure 35 it can be seen that the HF-current interruption is determined by the competition between the available UHF-TRV (U_m) and the reignition voltage U_r. Since the latter is proportional to the cold breakdown voltage U_b, the important conclusion can be drawn that materials that show good dielectric strength are also succesfull in interrupting HF-current. Only at high breakdown voltages the thermally dominated regime sets in and a more complex picture (as shown in the model) is necessary.

5.3 The maximum interruptable di/dt

Considering dielectrically dominated reignitions, with (15) and (32) the commonly accepted criterion of maximum interruptable di/dt can be written as:

$$\left|\frac{di}{dt}\right|_{max} = \frac{\alpha_0 U_b}{f_p L_{hf}} \tag{36}$$

from which it can be clearly seen that it is dependent on the 'cold' breakdown voltage U_b (as given in (23) and (24)) and dependent on the circuit by L_{hf} and f_p. For Cu, for which the dielectric reignition behaviour is absolutely dominant, the measured $|di/dt|_{max}$ and the $|di/dt|_{max}$ calculated from (36) are shown in figure 36.

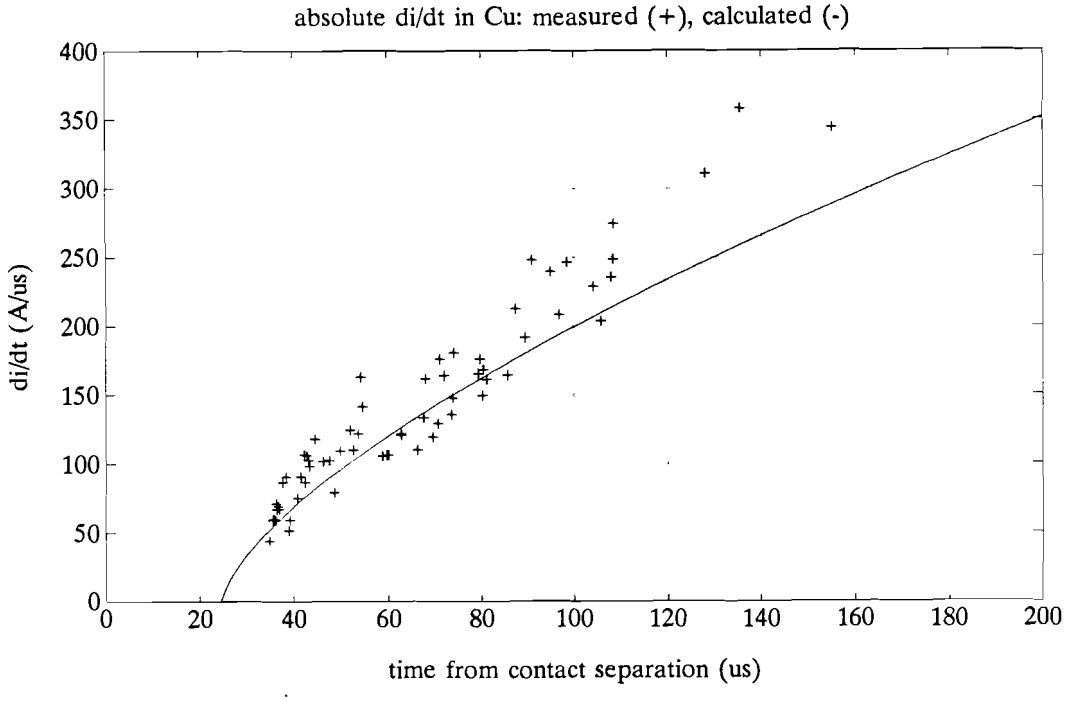

figure 36: measured maximum interruptable di/dt in Cu

It is clear that $|di/dt|_{max}$ is far from a constant in contrary to the breakdown voltage reduction factor. This can be seen from figure 37 where the breakdown voltage reduction factor for Cu is plotted as a function of the time from contact separation.

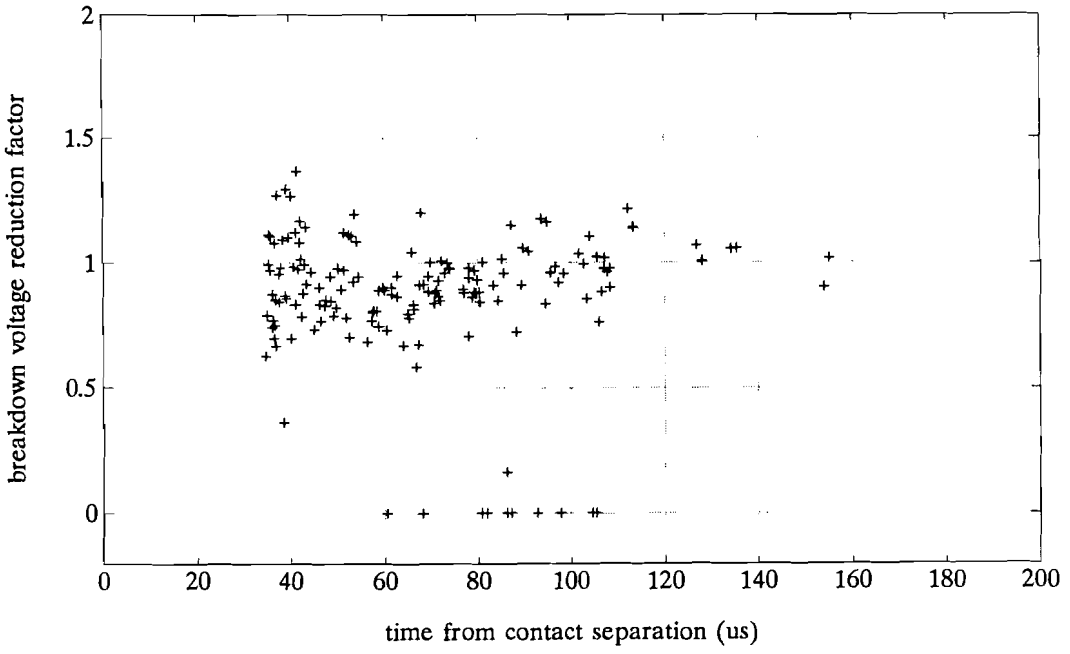

figure 37: reduction factor for Cu as a function of time from contact separation

5.4 The simulation methods

In the simulation methods described in [2] and [3] the reignitions are only determined by dielectric processes. Also the 'cold' recovery voltage is assumed to be a straight line and the breakdown voltage reduction factor is assumed to be a constant. The latter assumption turned out to be true for the dielectrically dominated reignitions. The 'cold' recovery can be described by the parameters found in 4.1. If the reignition phenomena are thermally dominated, the simulation methods have to be expanded by the thermal reignitions using the model shown in 5.2. First the 'rough' approximation of the thermal behaviour by i_{th} can be used. Later this could be replaced by a probability function based on the result in figure 26 on page 31.

In [2] a small influence of the breakdown voltage reduction factor was found, but in [3] it is concluded that the length of the arcing time during the HF-reignitions is important for the appearance of virtual current chopping. From 5.2 it has become clear that the HF-current can continue for a longer time than in the case of only dielectric reignitions.

6. CONCLUSIONS

- The speed of dielectric recovery of the various contact materials (Cu, CuCr, AgWC, CuW, CuBi and CuTeSe) shows a large variety. The fastest dielectric recovery (about 80V/μs) was found for Cu. The slowest recovery was found for CuTeSe (about 11V/μs). The speed of recovery for the other contact materials was between these two extremes.

- From the measurements done with a synthetic circuit, a small polarity effect of the 50Hz current on the reignition behaviour was found. Since our synthetic circuit forms a worst case concerning the 50Hz current influence, due to a very high rate of current decline towards current zero, the effect of prior 50Hz arcing in realistic circuits is negligible for low 50Hz currents (100A).

- Continuation of HF-arcing after breakdown of the gap is observed in three different manners:
  - thermal: one further HF-current half sine ('a reignition') without any perceptible rise of voltage (< 100V)
  - dielectric: a reignition appears when a certain voltage level is reached (5 - 15kV)
  - delayed: a reignition appears after the maximum of the TRV is reached

  For Cu and CuCr, about 90% of the reignitions is dielectric, for AgWC, CuW, CuBi and CuTeSe 26% to 45% is dielectric and 48% to 66% is thermal. Delayed reignitions only occur in CuCr, AgWC, CuW and CuTeSe.

- It was found that the breakdown voltage of the gap at HF-current zero is reduced with respect to the extrapolated cold breakdown voltage. This is due to HF-arcing, and can be quantified with a breakdown voltage reduction factor. This factor is either very close to zero (for which thermal reignitions result) or close to one (for which dielectric reignitions appear), depending on the preceding HF-current amplitude.

- The probability of occurrence of thermal reignitions is dependent on the preceding HF-current amplitude for AgWC, CuW, CuBi and CuTeSe. Below about 60A, most reignitions are of the dielectric type; above this threshold current thermal reignitions prevail. Cu and CuCr do not show such a tendency.

- For overvoltage generation, the duration of the HF-arcing periods is important. Below a certain threshold reignition voltage, the HF interruption is determined by dielectric processes. Above this threshold, thermal behaviour determines the HF-interruption. Generally, the duration of HF-arcing is longer in the thermally dominated mode. The measurements presented in this report are dominated by the dielectric behaviour.

- As long as reignitions are determined by the dielectric mode as found in this study, the occurrence of previous thermal reignitions is irrelevant. Nor is it necessary to distinguish between the two.

- For simulation the appearance of delayed reignitions is not relevant due to its isolated and single occurrence.

- A model is presented in which the thermal and dielectric reignition behaviour is integrated. This model can be used for simulation of vacuum interrupter behaviour with respect to overvoltage generation in a complete motor circuit. This simulation has to point out which contact material is suited best to avoid multiple reignition overvoltages in inductive circuits.

- **Materials that show good dielectric strength are also succesfull in interrupting HF-current. This is proved by measurement with all six contact materials. Hence it is not necessary to make a distinction between dielectric strength on the one hand and HF-current interruption capability on the other hand. The present study has proven their equivalence. Only at high breakdown voltages the thermally dominated regime sets in and a more complex picture (as shown in the model) is necessary.**

- The maximum interruptable di/dt is far from a constant and dependent on the circuit. Therefore, it is not suited to be used as an interruption criterion for HF-current. The description with the breakdown voltage reduction factor is better.

- Shielding of the measured signals during HF-reignition measurements in vacuum interrupters is unavoidable. The use of electronics should be avoided, unless shielded properly.

7. RECOMMENDATIONS FOR FURTHER RESEARCH

- The mechanism which causes a delayed reignition is unknown. It is expected that the post arc currents in combination with the UHF-TRV cause sufficient energy input into the ex-arc path to result in a reignition. If this is the case, delayed reignitions are thermal too. Therefore post arc current measurements should be done in AgWC, the metal with the highest relative appearance of delayed reignitions. The result can be compared with for example Cu, which shows no delayed reignitions at all.

- The reignition behaviour described in this report is measured for only one frequency of the HF-current. It could also be measured for various frequencies to investigate if the described behaviour is only dependent on the precedent current amplitude or also on the frequency.

- Direct evidence should be obtained in order to verify the dependence of the di/dt interruption criterion on circuit parameters.

- The influence of the UHF-TRV: in the model, the maximum value of the UHF-TRV is attributed the most important role. This assumes that the recovery processes after HF-current zero are slower than the risetime of the UHF-TRV. This could be verified by post-arc current measurements.

- The HF interruption model allows a more refined algorithm for overvoltage simulation programs, taking into account specific thermal and dielectric material parameters. A statistical interpretation of the breakdown reduction factor may approximate reality better than the 'discrete' model presented here.

8. REFERENCES

[1] Smeets, R.P.P., TUE diktaat college vermogensschakelaars in de elektriciteitsnetten, 1991.

[2] van Oostveen, J.P., 'Berekeningen aan overspanningen bij het schakelen in een motor testcircuit met vacuümschakelaars, Toepassing van de Nodal Matrix Admittance methode', M.Sc. thesis EG/92/640, TUE 1992.

[3] Kardos, R.C.M., 'Berekeningen aan overspanningen bij het schakelen in een motor testcircuit met vacuümschakelaars, Toepassing van de netwerkreductie methode', M.Sc. thesis EG/92/639, TUE 1992.

[4] Smeets, R.P.P., R.C.M. Kardos, J.P. van Oostveen, R.G.C. Dirven, H.Q. Li, E. Kaneko, 'Essential parameters of vacuum interrupter and circuit related to the occurrence of virtual current chopping in motor circuits', IEE Japan Power & Energy '93 proceedings, paper number E27.

[5] Ding, Bingjun, Hongqun Li, Xiaotian Wang, Jimei Wang, 'Critical temperatures of contact materials', IEEE Transactions on components, hybrids, and manufacturing technology, vol.15, no.1, february 1992, p.118-120.

[6] Laan, P.C.T. v.d., A.P.J. van Deursen, TUE collegediktaat EMC.

[7] Smeets, R.P.P., 'Multiple reignition in vacuum interrupters; part 2: Experimental investigations in CuCr and AgWC interrupters', internal report Toshiba.

Appendix A: Equipment used

HV-probe	Tektronix P6015 probe, attenuation ratio 1000:1 (variable by about 9%), input resistance 100MΩ (±3%), input capacitance approx. 3pF, maximum input voltage 20kV (DC or RMS) 40kV (pulse, maximum duty factor 10%, maximum pulse duration 0.1s), band-pass DC to 75MHz (-3dB), rise time approx. 4.67ns, temperature range -10°C to 55°C, length of interconnecting cable 10ft.
current transformer	Pearson Electronics, Inc. model no.110, output 0.1V/A (reduced to half by 50Ω termination), maximum peak current 5,000A, rise time 20ns, IT_{max} 0.5Asec, maximum RMS current 65A, approx. 3dB pt. 1Hz (low) 20MHz (high)
capacitor charger	N.V. Diode Utrecht, Hoogspannings Condensatorlader serieno.2, in: 220V/50Hz uit: 0-20kV/DC/100mA, TUE registration EH533 PS09
function generator	Wavetek Triggered VCG model 112, serial no. 086442, Wavetek San Diego California, TUE registration EH 398 GF01
oscilloscope	Lecroy dual 125MHz, model 9400. sensitivity 5mV/div to 5V/div (1MΩ), bandwidth DC 0-125MHz (-3dB), input impedance 1MΩ; < 30pF, maximum input voltage 250V, 1 AD-convertor per channel, 8-bit, 100Msamples/sec simultaneous, memory 32,000 8-bit words per channel, timebase 2ns/div to 100sec/div.

Acknowledgement

I would like to thank all the people who made it possible for me to do the work at the Energy Systems group of the Faculty of Electrical Engineering, which I enjoyed very much. Especially I would like to thank Mr. Hongqun Li and Mr. R. Smeets for their scientific and technical support, Mr. J. Vossen, Mr. L. Wilmes and Mr. A. v. Staalduinen for their technical support and Toshiba for its financial support. Also I would like to thank my family and friends for their support and understanding.